QTL mapping and transcriptome analysis of Sclerotinia-resistance in the wild cabbage species Brassica oleracea var. villosa

Thomas Bergmann
Molecular Phytopathology and Biotechnology, Christian Albrechts Universität zu Kiel
Jan Menkhaus
Molecular Phytopathology and Biotechnology, Christian-Albrechts-Universität zu Kiel
Markus Schemmel
Molecular Phytopathology and Biotechnology, Christian-Albrechts-Universität zu Kiel
Wanzhi Ye
Molecular Phytopathology and Biotechnology, Christian-Albrechts-Universität zu Kiel
Mario Hasler
Christian Albrechts Universität zu Kiel: Christian-Albrechts-Universitat zu Kiel
Steffen Rietz
NPZ Innovation GmbH
Gunhild Leckband
NPZ Innovation GmbH
Daguang Cai (dcai@phytomed.uni-kiel.de)
Christian-Albrechts-Universitat zu Kiel https://orcid.org/0000-0002-1816-6389

Research Article

Keywords: Sclerotinia sclerotiorum, Brassica oleracea, sclerotinia stem rot, SNP microarray, QTL, RNAseq

Posted Date: March 17th, 2021

DOI: https://doi.org/10.21203/rs.3.rs-309600/v1

Abstract

Oilseed rape (*Brassica napus*) is one of the most important oil-producing crops worldwide. The narrow gene pool of oilseed rape hampers its resistance breeding. Sclerotinia stem rot (SSR), caused by *Sclerotinia sclerotiorum*, is one of the most destructive diseases in many oilseed rape growing regions, worldwide. So far, no effective genetic source of resistance to *S. sclerotiorum* in *B. napus* germplasm is available, and yet knowledge of molecular plant-fungal interactions is limited. To identify new resistance source against SSR, we generated a segregating F_2 population for *Sclerotinia* resistance with 510 individuals from an interspecific cross between the resistant *B. villosa* (BRA1896) and a wild susceptible *B. oleracea* (BRA1909). Genetic mapping using a 15k Illumina Infinium SNP-array resulted in a high-density genetic map that contains 1,118 markers and spans a total genetic length of 792.2 cM. QTL-analysis identified 7 QTLs for Sclerotinia-resistance and 5 QTLs for trichome-phenotype, which explain up to 16.85 % and 34.45 % of corresponding phenotypic variance, respectively. Although a partial co-localization of major QTLs for trichome-phenotype and Sclerotinia-resistance was given, no functional association between these two traits could be validated. In addition, comparative RNAseq analysis suggests that activation of JA- and ethylene-mediated responses plays a central role in the Sclerotinia-resistance, associated with a stronger plant immune response, depressed cell death and elevated phytoalexin biosynthesis in *B. villosa*. Our data demonstrate that the wild *Brassica oleracea* complex represents a novel and unique genetic source of *Sclerotinia* resistance for breeding resistant oilseed rape against SSR.

Key Message

QTLs for Sclerotinia-resistance and trichomes were identified in *B. villosa,* offering a unique genetic source of Sclerotinia-resistance for breeding resistant oilseed rape against SSR.

Introduction

The necrotrophic fungus *Sclerotinia sclerotiorum* (Lib.) de Bary, a soil-borne fungal pathogen, causes the sclerotinia stem rot disease (SSR) in its host. The fungus embraces a broad spectrum of host plants with more than 400 species, including many economically important crops (Boland and Hall 1994, Bolton et al. 2006). The SSR overwinters as sclerotia in the soil. In spring, apothecia growing on sclerotia carpogenically germinate producing ascospores that are released into air currents and deposited to the petal and stem axil of its host plants. When conditions are favorable, the fungus starts to grow and infect the healthy stem tissue. The pronounced virulence of the fungus is attributed to among others a broad repertoire to produce cell-wall degrading enzymes, phytotoxins, and secreted effector-proteins (Amselem et al. 2011, Derbyshire et al. 2017). Most common symptoms are bleached lesions traversed by white mycelium in the stem or branch tissues and the formation of black sclerotia inside the infected tissue (Bolton et al. 2006). SSR is one of the most destructive diseases in many oilseed rape cultivation areas worldwide. The tremendous increase in cultivation area of oilseed rape in combination with shorter crop rotation cycles favored SSR dispersal over the past decades. Stems of infected plants tend to burst and shatter. The weakened stem stability and resulting lodging of the plants can cause severe yield and quality losses in oilseed rape cultivation (Derbyshire and Denton-Giles 2016). Resistance to Sclerotinia is mainly measured via leaf-, petiole-, or stem-inoculations on the basis of Zhao et al. (2003, 2004). Studies attempting to assess correlations between the different resistance traits reported contradictory results (Mei et al. 2011, Mei et al. 2013, Uloth et al. 2013, You et al. 2016, Taylor et al. 2018) and more effort is needed to determine their genetic link. Though SSR can be effectively controlled by application of fungicides (Derbyshire and Denton-Giles 2016) the increasing restriction of fungicide use due to its potential environmental and health hazards and the emergence of resistant isolates (Wang et al. 2014, Zhou et al. 2014) ask for alternative control strategies, worldwide. Breeding for resistant varieties is an important method in plant disease management. But, genetic resistance against SSR is generally lacking in the *B. napus* gene pool (Derbyshire and Denton-Giles 2016). To date, few genotypes that feature partial SSR-resistance are available (Zhao and Meng 2003, Wang et al. 2004, Taylor et al. 2015). Quantitative trait loci (QTL) for SSR-resistance have been reported in various *B. napus* mapping populations (Zhao and Meng 2003, Zhao et al. 2006, Yin et al. 2010, Wu et al. 2013, Wei et al. 2014, Behla et al. 2017) and genome-wide association studies (GWAS) identified single-nucleotide polymorphisms (SNPs) associated with SSR-resistance in numerous *B. napus* accessions (Gyawali et al. 2016, Wei et al. 2016, Wu et al. 2016). These studies report useful sources of partial SSR-resistance in the narrow oilseed rape gene pool. Efforts have been made to transfer high SSR-resistance from species intercrosses to the primary gene pool of *B. napus* (Chen et al. 2007, Garg et al. 2010). The *B. oleracea* complex, including *B. incana*, *B. rupestris*, *B. insularis*, and *B. villosa*, was identified as valuable pool of high SSR-resistance (Mei et al. 2011, Taylor et al. 2018). Mei et al. (2013) identified QTLs for SSR-resistance in a mapping population from an interspecific cross

between the wild *B. incana* (highly resistant) and the cultivated *B. oleracea* var. *alboglabra* (susceptible) and partially transferred this resistance via marker assisted selection (MAS) into the *B. napus* gene pool (Mei et al. 2015, Ding et al. 2019a, Mei et al. 2020). Comparative transcriptome analysis in the wild *B. oleracea* species linked this resistance to an early perception of the pathogen followed by a rapid release of reactive oxygen species (ROS) modulated by Ca^{2+} signaling pathways and an early suppression of Sclerotinia virulence genes (Ding et al. 2019b). These studies highlight the *B. oleracea* gene pool as important source for introgression of improved resistance to Sclerotinia into the primary gene pool of *B. napus*. Herein, we present results from phenotypic and genetic analyses on a segregating F_2-population from an intercross between the wild *B. villosa*, highly resistant to Sclerotinia, and the wild, susceptible *B. oleracea* var. *oleracea*. For the first time, we report QTLs for Sclerotinia-resistance and trichome-phenotype in the genome of *B. villosa*. In addition, the comparison with previously identified QTLs in the wild *B. incana* (Mei et al. 2013, Mei et al. 2017) allows for evaluating the resistance mechanisms existing in different Brassica species. Our genetic studies are complemented by an integrated reference- and *de novo*-based comparative transcriptome profiling 8 hours post inoculation (hpi), providing unique insights into the early defense response in the resistant *B. villosa*. We identified 58 *B. villosa*-specific significantly upregulated defense-related genes that are absent in the reference genome of *B. oleracea* and demonstrate that the distinct activation of the signaling pathways by jasmonic acid (JA) and ethylene (ET) plays a pivotal role in Sclerotinia-resistance and is associated with a strong immune response, a negative regulation of cell death, and an elevated phytoalexin biosynthesis.

Materials And Methods

Plant material and population structure

The seeds of *B. oleracea* (BRA1909) and *B. villosa* (BRA1896) were obtained from the Institute of Plant Genetics and Crop Plant Research (IPK) in Gatersleben, Germany. A segregating F_2 population with 510 individuals from an interspecific cross *B. villosa* x *B. oleracea* was divided into two mapping populations with 252 and 258 F_2-individuals, referred to as Population A and B, and cultivated under greenhouse conditions. From Population A, 234 F_2-plants were once evaluated for Sclerotinia-resistance via the detached leaf- and petiole-assay, from these 187 were selected for genotyping with the *B. napus* 15k Illumina Infinium SNP-chip. From Population B, 258 F_2-plants were evaluated once via the detached leaf- and petiole-assay. From these, 184 individuals were selected and genotyped. The phenotypic data from the genotyped Population B was re-evaluated with the leaf- and petiole-assay under greenhouse conditions twice. After resistance evaluation, 171 genotyped individuals in Population B were scored according to their trichome-phenotype.

Resistance screening and population comparison

Resistance evaluation was performed with the detached leaf- and petiole-assay (Zhao et al. 2004, Mei et al. 2011). We used a *S. sclerotiorum* strain originally isolated from an oilseed rape field in Chongqing, China (Mei et al. 2011). The fungus was cultured on potato-dextrose agar (20 g/l PDB, 15 g/l Bacto agar) plates with a pH of 5.6 at 21°C and transferred to a new PDA plate 2 days before inoculation. At least three plugs with actively growing mycelia were stamped out with a cork borer (d = 0.8 cm) and placed on the detached leaves with the mycelia-site facing the leaf-surface. The 3rd and 4th leaves (counted from the apical meristem) and their petioles were used for inoculation. PDA-plugs with actively growing Sclerotinia-mycelium were fixated with 1 ml pipette tips on the open cut of the petioles. Detached leaves and petioles were placed in a tray with wetted paper towel placed around open cut surfaces and sealed with foil. Leaf-lesion area and petiole-lesion length were measured two days post inoculation (dpi). The leaf-lesion area was calculated with the equation I, where ‘a’ equals the semi-major axis and ‘b’ indicates the semi-minor axis of a lesion ellipse.

Equation I: Leaf-lesion area [mm^2] = $\pi * a * b$

The mean leaf-lesion and petiole-lesion value was calculated for each individual plant. Lesion values of the parental plants were used to characterize F_2-individuals for their resistance in the whole population screenings. Plants with lesion values smaller than that of the resistant parent (*B. villosa*) were classified as ‘resistant’ while plants with lesion values larger than that of the susceptible parent (*B. oleracea*) were classified as ‘susceptible’. Plants with lesion values between those of *B. villosa* and *B. oleracea* were

defined as ‘intermediate’. Leaf- and petiole-lesion distributions from Population A and B were compared with relativized lesion values via equation II based on the parental lesion values in each population, respectively.

$$\text{Equation II: } \frac{(Lesion_{Single\ plant} - Lesion_{BRA1896})}{(Lesion_{BRA1909} - Lesion_{BRA1896})}$$

The relative value of *B. villosa* (BRA1896) is equal to zero (0) while the relative value of *B. oleracea* (BRA1909) is equal to 1 in both populations. Thus, plants with negative values correspond to the ‘resistant’ class, plants with positive values between 0 and 1 correspond to the ‘intermediate’ class, and values > 1 correspond to the ‘susceptible’ class in both populations.

Trichome screening in Population B

B. villosa is a densely haired and *B. oleracea* is a glabrous Brassica species. 171 individuals from Population B were screened for trichome-phenotypes on the basis of Mei et al. (2017) and classified into five trichome-groups from ‘0’ (completely hairless) to ‘4’ (densely haired). Individuals were scored according to the intensity of the trichome-layer on the leaf and petioles. Each tissue showing visible trichomes was scored with one point (max. two points). A dense trichome-layer as seen on *B. villosa* was scored with an additional point for each tissue (max. two points).

Trypan blue staining

Detached leaves of *B. villosa* and *B. oleracea* were placed in petri dishes, inoculated with PDA-plugs of actively growing Sclerotinia and sealed with Parafilm. After 2 dpi, leave tissue of the junction between necrotic and non-necrotic material was hand-dissected in small rectangles, placed into petri dishes and stained with Trypan blue staining solution according to Fernández-Bautista et al. (2016). Samples were visualized and taken with a SteREO Discovery.V20 microscope (Carl Zeiss AG, Oberkochen, Germany), an AxioCam MRc microscope-cam (Carl Zeiss AG, Oberkochen, Germany), and the AxioVision software (v. 4.8.2; Carl Zeiss AG, Oberkochen, Germany).

Statistical analysis

All statistical analyses were performed via the R software (v.3.6.3; R Core Team 2019). Data handling in R was mainly performed with the dplyr package (v.1.0.2; Wickham et al. 2019). Parental lesions in each population were compared via a linear model. Analysis of variance (ANOVA) was followed by multiple contrast tests with the multcomp package (v.1.4-15; Hothorn et al. 2008). Pearson’s correlation analysis was performed between leaf- and petiole-lesions in each inoculation-assay. The association between trichome-phenotype and Sclerotinia-resistance in Population B was analyzed via a one-way ANOVA. Post-hoc multiple comparisons between the lesion mean of each trichome-group to the grand mean of all groups were performed with the multcomp package (Hothorn et al. 2008). Figures were created via the ggplot2 package (v.3.3.2; Wickham 2016). Please see the ‘code availability statement’ for more information.

Genotyping and genetic map construction

Genomic DNA was isolated from leaves following the CTAB protocol (Rogers and Bendich 1985). DNA was resolved in HPLC-H_2O and DNA quality and concentration was determined on 1 % agarose gel with Lambda-DNA (Thermo Fisher Scientific, Massachusetts, USA) and the Image Lab Software (Bio-Rad Laboratories, California, USA). Genomic DNA (20 ng/µl) from each plant were loaded onto 96-well plates and send to TraitGenetics (Gatersleben, Germany) for genotyping with the Illumina® Infinium BeadChip technology (Illumina, California, USA) and the 15k Brassica chip (TraitGenetics, unpublished). The chip carries a total of 13,714 SNP markers. All SNP-marker were locally searched against the *B. oleracea* ‘TO1000’ reference genome (Parkin et al. 2014) retrieved from Ensembl Plants (Bolser et al. 2016) via BLAST+ (v.2.8.1; Altschul et al. 1990, Camacho et al. 2009) with the following options: -evalue 1e-5, -max_target_seqs 2, -max_hsps 1, -outfmt 6. Raw SNP-alleles were transformed into A/B/H-alleles via custom-written python code. The genetic map was constructed with the R/qtl package (v.1.46-2; Broman et al. 2003). Markers with distorted segregation patterns were filtered out based on a p-value < 1e-10 from the implemented chi-square test and arranged into linkage groups (min. LOD ≥ 8; max. recombination fraction = 35 %). The linkage groups were ordered with the implemented Haldane map function (assuming no crossover interference) and the ‘geno.crosstab’-function. The linkage groups were assigned to the chromosomes via the best hits from the local BLAST-search.

QTL analysis for Sclerotinia-resistance and trichomes

The QTL analysis was performed with the R/qtl package according to the workflow described in Broman and Sen (2009). First, both populations were separately screened for QTLs. The trichome-group in Population B was excluded as covariate in the analysis after no significant interaction between Sclerotinia-resistance and the trichome-phenotype was identified. The populations were screened for QTLs in three steps. A single-QTL model scan ('scanone'-function) was performed with the Haley-Knott regression (method = 'hk') followed by a scan with a non-parametric model, which considers the rank-based phenotypes (model = 'np'), when the first scan detected no QTLs. Peak-markers of identified QTLs were used as covariates in the single-QTL model to scan for additive and interactive effects of these markers to other loci followed by a two-dimensional QTL-scan considering epistatic effects. A multiple-QTL model was set up according to the identified loci from the scans and screened for additional ('addqtl'-function) and interacting ('addint'-function) QTLs. The model was adjusted and finally fitted with the forward/backward model selection algorithm with the Haley-Knott method via the 'stepwiseqtl'-function. The effect and amount of explainable phenotypical variance by each QTL was estimated with an ANOVA of the final multiple-QTL model. QTL-intervals were estimated with the Bayes credible method. QTLs with overlapping intervals were classified as common QTL. The significance thresholds were determined via genome-scan-adjusted p-values based on permutation tests (10,000 permutations for the single-QTL scans; 2,000 permutations for the two-dimensional scans). Phenotypes of identified QTLs from both populations were transformed into relative lesion values on the basis of Equation II and merged for a fine mapping. Please see the 'code availability statement' for more information.

Comparative RNAseq analysis

Total RNA was isolated from Sclerotinia-inoculated and mock-inoculated petioles of *B. villosa* and *B. oleracea* 8 hpi with the innuPREP Plant RNA Kit (Analytik Jena AG, Jena, Germany) according to the manufacturer's recommendation. Three biological replications each consisting of pooled eight petioles from four plants were employed. RNAseq analysis was performed by Novogene (Bejing, China) on the Illumina HiSeq 4000 system. Transcriptomic analysis was performed with reference-based and *de novo*-based RNAseq software tools. Briefly, raw reads were processed by removing reads with an average quality less than Q30 (AVGQUAL: 30) via the Trimmomatic software (v.0.39; Bolger et al. 2014). Clean reads were aligned to the *B. oleracea* 'TO1000' reference genome (Parkin et al. 2014) and assembled to a transcriptome via the 'new Tuxedo' protocol including HISAT2 (v.2.2.0; Kim et al. 2019) and StringTie (v.2.1.4; Pertea et al. 2015) as described in Pertea et al. (2016). SAM files were sorted and converted to BAM files via SAMtools (v.1.9; Li et al. 2009). The gff utilities (Pertea and Pertea 2020) 'gffread' (v.0.11.8) and 'gffcompare' (v.0.11.6) were used to extract reference transcript sequences and to retrieve transcriptome assembly statistics.

For differentially expressed gene (DEG) analysis, the gene count matrix was extracted with the enclosed python script in the StringTie software package. Unmapped reads from the reference transcriptome assembly were then extracted from the BAM files via 'samtools view' with the following parameters: -f 12; -F 256. Unmapped BAM files were converted to fastq format via the 'bamtofastq' utility from BEDtools (v.2.29.2; Quinlan and Hall 2010) and re-aligned to the *S. sclerotiorum* '1980' genome (Amselem et al. 2011). Unmapped reads that neither aligned to *B. oleracea* nor to *S. sclerotiorum* were then re-converted to fastq format and assembled *de novo* via Trinity (v.2.9.0; Grabherr et al. 2011). Counts of the *de novo* transcripts were estimated via RSEM (v.1.3.3; Li and Dewey 2011). The *de novo* transcript count matrix was filtered for transcripts with at least 10 counts in each of the three biological replications within a sample. The filtered transcript matrix was added to the gene count matrix from the reference transcriptome assembly. DEG analysis was performed with the merged count matrix via DESeq2 (v.1.26.0; Love et al. 2014). Genes were considered as significantly differentially expressed with an adjusted P-value of < 0.05. The calculation of the sample-to-sample distance matrix and the principal component analysis (PCA) are based on the regularized log-transformed counts in DESeq2. Samples were checked for outliers by Cook's distance. For each gene, the major isoform, calculated by the averaged transcript fragments per kilobase million (FPKM), was used for functional annotation. Graphical illustrations and data conversions were performed in R via ggplot2 (Wickham 2016) and dplyr (Wickham et al. 2019). Please see the 'code availability statement' for more information.

Functional annotation and gene enrichment analysis

The TransDecoder software (v.5.5.0; https://github.com/TransDecoder/TransDecoder/wiki) was used to convert transcript sequences into protein sequences and to identify functional protein-domains. Briefly, longest open reading frame prediction was performed via the 'TransDecoder.LongOrfs' tool. The likely protein-coding regions were used for a homology-based coding region

identification in Pfam (El-Gebali et al. 2019) via the HMMER software (v.3.2.1; http://hmmer.org/) and in a protein sequence database of Arabidopsis (organism: 3702) downloaded from Uniprot (The Uniprot Consortium 2019) via the BLASTp+ software and the following options: -evalue 1e-5, -max_target_seqs 1, -max_hsps 1, -outfmt 6. The Pfam and BLAST+ results were integrated into the final coding region prediction via the 'TransDecoder.Predict' tool. Gene ontology (GO) annotations of the Brassica transcripts were retrieved from their closest homolog in Arabidopsis via the database from KOBAS 3.0 (Xie et al. 2011). Additionally, all transcripts were blasted against the *B. oleracea* (Taxid: 109376) Refseq database. Gene enrichment analysis was performed with the goseq package (v.1.38.0; Young et al. 2010) taking the gene length bias of RNAseq into account. The p-values were adjusted via the false discovery rate method (Benjamini and Hochberg 1995) and GO terms were considered statistically enriched with a FDR ≤ 0.05. The comparative GO analysis was performed and output tables were created with custom-written R-scripts. Heatmaps were created with the ComplexHeatmap package (Gu et al. 2016). Please see the 'code availability statement' for more information.

Quantitative gene expression analysis

RNA was isolated at 8 hpi and 16 hpi as described before from three independent biological replications of Sclerotinia- and mock-inoculated petioles from *B. villosa* and *B. oleracea*. 500 µg of RNA of each sample was treated with RNase-free DNaseI (Thermo Fisher Scientific, Massachusetts, USA) and transcribed to cDNA with the RevertAid First Strand cDNA Synthesis Kit (Thermo Fisher Scientific, Massachusetts, USA) according to the manufacturer's instructions and diluted 1:5. Two microliters cDNA were mixed with 18 µl Master Mix as described in the manual of the qPCRBIO SyGreen Mix (PCR Biosystems Inc., Pennsylvania, USA). qPCR was performed on a CFX96 Touch Real-Time PCR Detection System (Bio-Rad Laboratories, California, USA). Conditions for the reactions were as follows: 3 min at 95 °C; 40 cycles of 95 °C for 15 s, 60 °C for 15 s, and 72 °C for 20 s. Relative quantification was calculated in relation to Actin7 (Bo3g005290) according to Pfaffl (2001), which showed a stable expression in the RNAseq. Analysis of primer efficacy was determined by a standard curve of pooled cDNA from all samples for each gene. Primer and their predicted targets in the RNAseq are provided in the supplement (Supplementary Data S6). Statistical analysis was performed via a linear model using generalized least squares with the nlme-package (Pinheiro et al. 2020). Sequencing of selected templates validated targets in the wild *B. oleracea* species. The log2-transformed gene expression from the qPCR data at 8 hpi was compared to the RNAseq data.

Results

Parental performance in the leaf- and petiole-assay

B.villosa (BRA1896) was identified as highly resistant to Sclerotinia compared to *B. oleracea* (BRA1909). Differences between the two species were highly significant ($p < 0.01$) in the petiole-assays in both populations and in the leaf-assay in Population A, but not significant in the leaf-assay in Population B (Fig S1). We observed noticeable differences in the fungal spread on infected leaves via Trypan blue staining. A dense and compact structured growth mainly within the necrotic tissue with a sharply delimited junction between healthy and infected tissue was characteristic for the susceptible *B. oleracea* (Fig. S2). In the resistant *B. villosa*, the fungal expansion was less structured, mainly centered on the leaf surface with no sharply delimited changeover between healthy and infected tissue and strongly pronounced infection cushions.

Evaluation of F_2-plants for Sclerotinia-resistance

In total, 234 F_2-plants in Population A and 258 F_2-plants in Population B were screened for Sclerotinia-resistance with the detached leaf- and petiole-assay. Leaf-lesion values in Population A ranged from 241.3 to 1452.4 mm^2 and petiole-lesion values from 19.5 to 55 mm. Leaf-lesion values in Population B ranged from 78.4 to 867 mm^2 and petiole-lesion values from 12.9 to 47.9 mm. Leaf- and petiole-lesion values showed a transgressive segregation in both populations for leaf- and petiole-resistance (Fig. 1). In total, 212 plants were classified as 'resistant', 181 as 'intermediate', and 99 as 'susceptible' in the leaf-assay. 72 F_2-plants were classified as 'resistant', 291 as 'intermediate', and 129 as 'susceptible' in the petiole-assay. The amount of 'resistant' F_2-plants in the leaf-assay was larger compared to the amount of 'resistant' F_2-plants in the petiole-assay. The leaf-lesion difference between the parental plants was smaller in Population B, resulting in a shift of the leaf-lesion distribution compared to Population A (Fig. S1c). The amount of plants classified as 'intermediate' (60 plants) decreased and more plants were classified as 'resistant' (121 plants) or 'susceptible' (77 plants) in Population B in the leaf-assay. The petiole-assay showed a similiar lesion-distribution in both populations (Resistant: 20 in Population A; 52 in Population B; Intermediate: 172 in Population A; 119 in Population B; Susceptible: 42 in

Population A; 87 in Population B), where the class of 'intermediate' represented the major fraction of F_2-plants. The oilseed rape variety 'Falcon' showed a high degree of susceptibility in both assays.

Association between leaf- and petiole-lesions

Pearson's correlation analyses revealed a weak significant positive correlation between leaf- and petiole-lesions (Population A = $p < 0.001$; Population B = $p < 0.01$) explaining about 28 % of variance in Population A and about 2 % of variance in Population B (Fig. 2a). The intersection of F_2-genotypes classified into common categories in the leaf- and petiole-assay was small in both populations (Fig. S3). Of all individuals, 47 out of 237 'resistant' individuals in either the leaf- or the petiole-assay were commonly classified as 'resistant' in both assays. 120 F_2-plants were commonly classified as 'intermediate' and 40 individuals were classified as 'susceptible' in both assays. All 207 individuals commonly classified as 'resistant', 'intermediate', and 'susceptible' from both populations were selected for genotyping. 164 individuals with mainly moderate variation between the three categories were additionally selected for genotyping. The correlation between leaf- and petiole-lesions in the genotyped individuals increased to 31 % of explainable variance ($r = 0.56$) in Population A and to 14 % of explainable variance ($r = 0.38$) in Population B (Fig 2B and C). Significant positive correlations ($p < 0.001$) were also identified in the 2nd and 3rd infection of the genotyped individuals in Population B with 25 % ($r = 0.50$) and 7 % ($r = 0.27$) of explainable variance, respectively (Fig 2D and E). The correlation increased with respect to the absolute lesion sizes.

Association between trichome-phenotype and Sclerotinia-resistance

A broad range of variation in the trichome-phenotype was observed in individuals of Population B (Fig. 3). Of the 171 screened F_2-individuals, 101 were hairy and 70 were glabrous. The chi-squared test showed a significant deviation ($X^2 = 23.16$, $p = 1.491e\text{-}06$) from a 3:1 segregation. The 101 hairy individuals were composed of 30, 23, 12, and 36 individuals classified as trichome-group '1','2','3', and '4', respectively. The association between the trichome-phenotype and the lesion size is shown in Fig 4. Trichome-group '4' was significantly associated with lower lesion values in the 2nd leaf- and petiole-assay ($p < 0.001$, $p < 0.05$) (Fig. 4B and E). Trichome-group '0' was significantly associated with higher lesions in the 2nd leaf-assay (Fig. 4B) and trichome-group '3' was significantly associated with increased lesions in the 3rd petiole-assay (Fig. 4F). A consistent trend between the trichome-groups and their level of Sclerotinia-resistance was not observed.

Construction of a high-dense genetic map

Genotypic data of 371 F_2-plants was combined to construct a common genetic map for both populations (Table S1). 8,646 SNPs from the Brassica 15k SNP-chip-array were uniquely aligned to the *B. oleracea* genome via the best hit from the local BLAST-search. The most SNPs (1,466) were aligned to chromosome C03 and the fewest (522) to chromosome C09. Ten F_2-individuals were discarded for genetic map construction due to considerable genotyping errors. 1,118 SNPs were polymorphic between the parents and ordered into a genetic map with 10 linkage groups with a total length of 784.9 cM and an average distance of 0.7 cM between adjacent markers. Linkage groups were assigned to the chromosomes of *B. oleracea* according to the local BLAST. Low marker coverage of C04 resulted in two separate linkage groups (C04a, C04b). Genetic positions of markers were concordantly with their assumed physical positions in the *B. oleracea* genome (Supplementary Data S4).

Identification of seven QTLs for Sclerotinia-resistance

Seven QTLs associated with resistance against Sclerotinia were detected with the single-QTL analysis (Table 1). No additional or interacting QTLs were detected with the two-dimensional or the 'stepwiseqtl'-function. The loci are allocated on chromosomes C01, C03, and C07, with two overlapping QTLs (pQTLa, l2QTLb) on C01, two (p1QTLb1, p3QTLb1) on C03, and two (p1QTLb2, p3QTLb2) on C07 representing a common QTL, respectively. pQTLa was detected via the petiole-assay in Population A with the peak at marker Bn-scaff_19564_1-p17934. The marker was mapped to Scaffold01187 (~ 23 kb). Flanking markers were Bn-scaff_15749_1-p118178 (26,828,052 bp) and Bn-scaff_16929_1-p495739 (29,084.454 bp). l2QTLb and l3QTLb were detected in the 2nd and 3rd leaf-assay in Population B. The peak of l2QTLb was detected at 51 cM between Bn-scaff_15747_1-p105633 (14,270,425 bp) and Bn-scaff_22790_1-p152675 (16,593,775 bp), which was the marker nearest to the peak. pQTLa and l2QTLb overlapped by ca. ~ 10 cM. Genetic distance between the peaks was 2 cM, corresponding to ca. 12.5 Mbp. The peak of l3QTLb was detected at marker Bn-scaff_16110_1-p976517 (47,351,349 bp) at 79.6 cM. p1QTLb1 and p1QTLb2 were identified via the 1st petiole-assay in Population B

and p3QTLb1 and p3QTLb2 were identified via the non-parametric method in the 3rd petiole-assay in Population B. The peak of p1QTLb1 was detected at 12 cM between the markers Bn-scaff_16614_1-p174856 (2,054,448 bp) and Bn-scaff_18936_1-p269153 (3,106,932 bp). Bn-scaff_16069_1-p4306874 (44,016,862 bp) was detected as peak-marker at 54.3 cM for p1QTLb2. p3QTLb1 was detected with a LOD of 3.22 below the LOD-threshold of 3.49 (p = 0.08) with the peak at 13.1 cM at marker Bn-scaff_18936_1-p269153 (3,106,932 bp). Peaks of p1QTLb1 and p3QTLb1 were separated by 1.1 cM and shared the same adjacent peak-marker (Bn-scaff_18936_1-p269153) and therefore declared as common QTL. Bn-scaff_16069_1-p2611780 (42,321,768 bp) was the nearest marker to the peak of p3QTLb2 with a physical distance of 1,695,094 bp to the peak of p1QTLb2 at 44,016,862 bp. l3QTLb showed a partial overlap of 4.6 cM, corresponding to 607.116 bp, at the end of the interval from p1QTLb2 but no overlap with p3QTLb2. The peaks between l3QTLb and p1QTLb2 were separated by 32.63 cM (3,334,487 bp). Two identical non-significant peaks were observed in the 1st and 3rd petiole-assay on C06 (Fig. S4B). An additional scan with the two-QTL model (y ~ p1QTLb1 + p1QTLb2) in the 1st petiole-assay increased the LOD from 2.79 to 3.53 below the LOD-threshold of 3.56 (p = 0.053). Both peaks from the 1st and 3rd petiole-assay on C06 were localized at 46.8 cM (35,415,831 bp) and 47.8 cM (35,610,420 bp) and showed a minor additive effect in Population B. The QTLs on C01 explained about 15.8 % (pQTLa) and 16.5 % (l2QTLb) of variance. The QTLs on C03 accounted for ca. 8.1 % (p1QTLb1) and 3.9 % (p3QTLb1) of explainable variance. The QTLs on C07 explained about 10.4 % (l3QTLb), 9.9 % (p1QTLb2), and 4.8 % (p3QTLb) of phenotypical variance, respectively. Alleles of *B. villosa* in pQTLa reduced the petiole-lesions on average from 42.61 mm to 34.96 mm, in l2QTLb from 710.94 mm^2 to 465.68 mm^2, in l3QTLb from 479.65 mm^2 to 447.82 mm^2, in p1QTLb1 from 31.18 mm to 26.52 mm, in p1QTLb2 from 31.31 mm to 26.37 mm, in p3QTLb1 from 27.49 mm to 23.61 mm, and in p3QTLb2 from 25.93 mm to 22.53 mm. Alleles from the susceptible *B. oleracea* were dominant in four of the seven identified QTLs.

Fine mapping of QTLs for Sclerotinia-resistance

Similar LOD-profiles between assays in both populations were observed (Fig. S4). Noticeable, several peaks were observed on chromosome C01 adjacent to pQTLa and l2QTLb from leaf- and petiole-assays in Population B and several non-significant peaks were observed on C02. The leaf-assay from Population A contributed to one peak on C08, which was not observed in any other assay (Fig. S4A). In order to increase the power and precision to detect QTLs, lesion values were transformed into relative lesions via Equation II with following modification: lesions of *B. villosa* and *B. oleracea* were replaced by lesion-values of the genotyped F_2-plants at the border of the 25 % and 75 % quantile in each assay, respectively. We merged the relative lesion values from the petiole-assay (pQTLa) in Population A with the relative lesion values from the 2nd (l2QTLb) and 3rd (l3QTLb) leaf-assay, as well as with the relative lesion values from the 1st (p1QTLb1/p1QTlb2) and 3rd (p3QTlb1/p3QTLb2) petiole-assay in Population B. The merged scans were performed with the Haley-Knott regression and are summarized in Table 1. The combined analysis increased the LOD and decreased the estimated intervals for all QTLs except for p1QTLb1/p3QTL and l3QTLb. The joint scan of phenotypes from pQTLa and l2QTLb (pAlB2) showed an additive effect that increased the LOD of pQTLa and l2QTLb from 6.2 to 10.7 with a peak at 50 cM (Fig. 5A). The estimated QTL-interval decreased to 7.1 cM (13,002,326 bp - 29,084,454 bp). The peak was detected between the flanking markers: Bn-scaff_15747_1-p105633 (14,270,425 bp) and Bn-scaff_22790_1-p152675 (16,593,775 bp). Other phenotype combinations did not increase the LOD on chromosome C01. Evidence for QTLs on C03 and C06 vanished completely. Peaks on chromosome C03 shifted to 91.8 cM (36,288,851 bp) and 88.5 cM (33,853,232 bp) but were not significant (Fig. 5B and C). The joint scan of phenotypes from pQTLa and l3QTLb (pAlB3) decreased the LOD of l3QTLb from 4.07 to 3.77 (Fig. 5D) and moved the peak to 80.5 cM at Bn-scaff_16110_1-p426547 (47,901,219 bp). The estimated QTL-interval increased from 9.16 cM to 14.54 cM (2,367,296 bp). The phenotypes from pQTLa exerted an equal additive effect to the phenotypes from p1QTLb2 (pApB1) and p3QTLb2 (pApB3) (Fig. 5E and F). LOD-scores increased from 4.56 to 5.29 for p1QTLb2 and from 3.78 to 4.41 for p3QTLb2. The peaks moved from 54.3 cM to 58 cM and from 46.9 cM to 59 cM, respectively. Nearest peak-markers were: Bn-scaff_16069_1-p4828119 (44,538,108 bp) and Bn-scaff_16110_1-p3674923 (44,652,843 bp). The estimated interval for p1QTLb2 decreased from 13.14 cM (2,062,672 bp) to 8.8 cM (1,470,303 bp) for pApB1 and increased for p3QTLb2 from 32.41 cM (5,817,550 bp) to 33.75 cM (5,619,756 bp) including the non-significant distal peak at the end of C07. The results on chromosome 7 indicate l3QTLb as separate QTL at the end of this linkage group.

Identification of QTLs for trichome-phenotypes

Five QTLs associated with trichome-development were identified (Table 1). The single-QTL analysis identified three genomic regions on C01 (t1QTLb), C04b (t2QTLb), and on C09 (t3QTLb). A single-scan controlling for the major QTL on chromosome C01 and a two-

dimensional QTL-scan indicated two additional loci on C03 (t4QTLb) and C07 (t5QTLb) with additive effects. A scan with the additive multiple-QTL model repeatedly detected the two QTLs with a LOD of 3.58 for t4QTLb and of 5.96 for t5QTLb (Fig. 6). The LOD of t4QTLb was at the level of the LOD-threshold (p = 0.058). Both QTLs were added to the model with additive effects. Significant epistatic interactions were not identified. The 'stepwiseqtl'-function confirmed the best fit of the five QTL-model with mainly additive effects. The main peak of t1QTLb was co-localized with the major QTL for Sclerotinia-resistance on C01 at 50 cM between the markers Bn-scaff_15747_1-p105633 (14,270,425 bp) and Bn-scaff_22790_1-p152675 (16,593,775 bp), and explained ca. 36.8 % phenotypical variance. The estimated interval was 5.76 cM (3,591,449 bp). The peak of t2QTLb was detected at Bn-scaff_16888_1-p1168071 (50,145,435 bp), accounting for 5.5 % of phenotypic variance. t3QTLb explained about 12.9 % of phenotypic variance with a peak at 7 cM between Bn-scaff_17526_1-p1667260 (2,112,449 bp) and Bn-scaff_17526_1-p952618 (2,827,091 bp). t4QTLb explained about 3.9 % of phenotypic variance. The peak was detected at marker Bn-scaff_16352_1-p1063388 (17,865,682 bp). The peak of t5QTLb was identified at 33 cM between Bn-A06-p24207308 (no position available) and Bn-A06-p24068524 (29,764,020 bp). Nearest left flanking marker to Bn-A06-p24207308 with a physical position was Bn-scaff_15754_1-p477663 (29,211,394 bp). t5QTLb accounted for 5.6 % of phenotypic variance.

Comparative transcriptome profiling

Hierarchical clustering and PCA analysis of the RNAseq samples showed a grouping according to species and treatment. 58 % and 39 % of variance between the samples were attributed to the species and the response to the treatment, respectively (Fig. S5A and B). Overall, 63,995 genes were identified in both species. We identified 6,630 up- and 1,829 downregulated DEGs in the resistant *B. villosa* and 7,209 up- and 3,566 downregulated DEGs in the susceptible *B. oleracea* at 8 hpi with Sclerotinia. Of these, 5,095 up- and 751 downregulated DEGs were common in both species (Fig. 7A). In total, 854 genes had a significant difference in their log2-fold change between the species as response to the inoculation. 542 genes had a positive log2-fold change difference, meaning a significant stronger induction in the resistant *B. villosa*, while 312 genes showed a significant stronger induction in the susceptible *B. oleracea* (Fig. 7B). We identified 111 GO terms that were commonly enriched in both species that addressed direct pathogen-induced reactions, such as a response to chitin (GO:0010200) and a response to fungus (GO:0009620). In both species, responses to ethylene (ET; GO:0009723) and to abscisic acid (ABA; GO:0009737) were significantly stronger enriched than responses to salicylic acid (SA; GO:0009751) and jasmonic acid (JA; GO:0009753). The ET-activated signaling pathway (GO:0009873) was 7 x 10^6-times more significantly enriched in the resistant *B. villosa* in comparison to *B. oleracea*. In the susceptible host, we identified a 50-times more significantly enriched response to SA (GO:0009751) and a three-times more significantly enriched response to JA (GO:0009753) in *B. oleracea*. Both species showed a highly significant (log10-FDR < -30) response to decreased oxygen levels (GO:0036293). The immune response (GO:0006955) was strongly addressed in both species, but 7.6 x 10^{11} times more significantly in the resistant *B. villosa*. Regulatory processes of the immune system (GO:0050776), a negative regulation of cell death (GO:0060548), and a positive regulation of defense response (GO:0031349), as well as a response to reactive oxygen species (ROS; GO:0000302) were specifically enriched in *B. villosa*. The resistant BRA1896 showed overall a strong increase in the primary metabolism (e.g., GO:0015979; GO:0016168; GO:0047899; GO:0009538) and in the phytoalexin metabolic process (GO:0052314; GO:0046217; GO:0052317). The susceptible *B. oleracea* showed a specific enrichment of the glycosinolate metabolic process (GO:0019757) and the ABA-activated signaling pathway (GO:0009738). The GO enrichment analysis of the 854 genes with significant differences in their log2-fold change expression revealed multifaceted transcriptomic strategies in the commonly enriched terms of both species due to the inoculation. For example, 53 genes associated with the hormone-mediated signaling pathway (GO:0009755) showed a significant difference in their expression between the two species as result of the inoculation. Further differences were identified in the signal transduction (GO:0007165; 94 genes), in the response to decreased oxygen levels (GO:0036293; 28 genes), in the response to ABA (GO:0009737; 42 genes), and in the ET-activated signaling pathway (GO:0009873; 17 genes). The complete results of the GO analysis for each species are in the supplementary data (Data S7 – S9). The detailed comparative analysis is available as report (see the 'code availability statement'). The RT-qPCR analysis of the phytohormone markers AOC3 (JA), ETR2 (ET), LOX3 (JA), NCED3 (ABA), PR1 (SA), and PDF1.2 (JA) confirmed the different activation of the hormone-mediated signaling pathways observed in the RNAseq (Fig. S6). AOC3 and LOX3 showed strong significant expression at 8 hpi and 16 hpi in the susceptible host, whereas a weaker non-significant expression was observed at both time points in *B. villosa*. Expression of PR1 showed strong variation and was higher in *B. villosa*, which was also observed in the RNAseq data. ETR2 was highly induced at both time points in the resistant *B. villosa* and showed an increase from 5.39-fold at 8 hpi to 8.57-fold at 16 hpi. A weaker non-significant gene expression was observed in *B. oleracea*. We observed a significant 9.38-fold and 12.1-fold expression of NCED3 at 8 hpi in *B. villosa* and *B. oleracea*. The expression decreased to non-significant 5.66-fold in *B. villosa* and increased

significantly to 18.61-fold at 16 hpi in *B. oleracea*. PDF1.2 showed a non-significant 2.36-fold and 1.14-fold expression at 8 hpi and a decrease to 0.03-fold and 0.44 at 16 hpi in the resistant and the susceptible host, respectively. The qPCR data at 8 hpi generally confirmed our RNAseq data (Fig. S7).

Identification of candidate genes in *B. villosa*

For candidate gene analysis, we focused on the major peak regions from pAlB2 (14,270,425 bp – 16,593,775 bp) and pApB1/pApB3 (44,538,108 bp – 44,736,714 bp) with left and right flanking markers next to the peak. Our transcriptome data revealed 242 genes with 19 and 44 DEGs in the resistant and susceptible host in the major peak area of pAlB2 (Supplementary Data S10). Four of the 242 genes had a significant difference in expression. The peak region of pApB1/pApB3 harbors 27 genes of which no gene showed a significant difference in expression between *B. villosa* and *B. oleracea* (Supplementary Data S11). Six and seven of the 27 genes were identified as differentially expressed in *B. villosa* and *B. oleracea*, respectively. Gene annotations varied from uncharacterized proteins to kinase like proteins. We did not identify genes with striking expression patterns between both species. Therefore, we set the focus to *B. villosa*-specific transcripts from the *de novo* assembly. Overall, 15,251 *de novo* transcripts were reconstructed from both species of which we identified 3,144 and 3,230 transcripts as DEGs. A comparison of the upregulated transcripts revealed 413 DEGs specifically upregulated in the resistant *B. villosa*. Of these, 110 DEGs are associated with response to stress (GO:0006950), 58 DEGs are associated with defense response (GO:0006952), 29 DEGs are related to immune system process (GO:0002376), and 56 DEGs are associated with a response to oxygen-containing compound (GO:1901700). A comparative gene expression analysis of the 58 DEGs associated with defense response revealed that most of these genes are specific to *B. villosa* (Fig. 7C, Supplementary Data S12). Nine of these 58 DEGs showed contrary expressions in *B. oleracea*.

Discussion

The petiole-assay is an efficient and reliable method to assess Sclerotinia-resistance

Both assays identified *B. villosa* as highly resistant to Sclerotinia, in accordance with previous observations (Mei et al. 2011, Taylor et al. 2018). The discrepancy observed between the petiole-assays and the leaf-assays is clearly attributed to different inoculation systems. We observed that a fast drying of PDA-plugs on the leaf-surface and irregularities of the leaf-surface severely impeded the inoculation process in some leaf-assay cases. In the petiole-assay, PDA-plugs are well protected from dehydration by the surrounding pipette tip, and the fungus can easily infiltrate the petiole via an open cut of the petiole tissue. A high degree of variation in leaf-architecture and trichome-phenotype was obvious in F_2-plants. Even within an individual plant, the leaf-lesion variation was higher than that in the petiole-assay. Noticeably, the comparison, of the lesion-distribution between Population A and Population B showed a similar number of ‘resistant’, ‘intermediate’, and ‘susceptible’ F_2-individuals in the petiole- but not in the leaf-assays. But the expected transgressive segregation was given in the petiole- and leaf-assay of Population A, and in the petiole-assay of Population B, in which the leaf-assay classified most plants (120 F_2-plants) as ‘resistant’. This reflects an overestimated proportion of ‘resistant’ F_2-individuals by the leaf-assay in Population B. Though the leaf inoculation is a well-established Sclerotinia-inoculation technique (Zhao and Meng 2003, Mei et al. 2011, Wu et al. 2013, Joshi et al. 2016), our data suggest that the petiole-assay (Zhao et al. 2004) is a more reliable, reproducible, and efficient tool for a large-scale screening for Sclerotinia-resistance. In consistence, Taylor et al. (2018) found no significant correlation between leaf- and stem-resistance in a set of wild Brassica species. Uloth et al. (2013) and You et al. (2016) found no association between leaf- and stem-resistance under field-conditions in diverse Brassica species. By contrast, a positive correlation between leaf- and stem-resistance under field- and controlled-environments by artificial inoculation was reported by Mei et al. (2011, 2013). Even though several factors can impair the leaf- and petiole-inoculation systems, an additive effect of the merged leaf- and petiole-phenotypes from Population A and B for the major QTL on C01 observed in this study strongly supports for a common genetic basis determining the leaf- and petiole-resistance in the wild *B. villosa*. A low power of the leaf-assay might be the cause for no other overlapping QTLs between both assays.

B.villosa is a unique source of Sclerotinia-resistance

The separate analysis of two mapping populations facilitated the identification of a minor QTL on chromosome C03 in Population B. In total, seven loci associated with Sclerotinia-resistance were identified in the genome of the wild *B. villosa*. The merged analysis of phenotypes from Population A and B, enabled a fine mapping of the QTLs on chromosomes C01 and C07. The phenotypes for pQTLa and l2QTLb showed a strong additive effect when combined with an increase of the LOD from 6.2 to 10.7. The QTL-interval

was narrowed down from 28 Mbp (l2QTlb) and 26 Mbp (pQTLa) to 16 Mbp and the peak was localized between 14,270,425 bp and 16,593,775 bp. For the QTL on chromosome C07, the fine mapping consequently reduced the distance between the peaks from p1QTLb2 and p3QTLb2 from 1,695,094 bp to 114,735 bp. An integrated analysis conducted by Li et al. (2015) physically mapped QTLs for Sclerotinia-resistance from several studies to the genome of *B. napus*. Most conserved QTLs for Sclerotinia-resistance in *B. napus* are located on chromosome C06 and C09. In this study, we got low evidence for a minor QTL only on C06 in Population B but could not validate it. This may because of different inoculation systems, materials, and markers used in the studies. In similar studies, Mei et al. (2013, 2017) produced and analyzed a mapping population from a cross between wild *B. incana* (resistant) and the cultivated *B. oleracea* var. *alboglabra* (susceptible). A major QTL for Sclerotinia-resistance on chromosome C09, which explain about 13.6 % of phenotypical variance, and a QTL on chromosome C01 were reported. Remarkably, the QTL on chromosome C01 in *B. oleracea*, ranging from 13 Mbp to 29 Mbp identified in this study perfectly matches the previously reported QTL from Mei et al. (2013) on chromosome C01 in *B. napus* (Li et al. 2015). Thus, comparison between the two QTL as well as their physical overlapping regions may provide more insights into the genetic basis for Sclerotinia-resistance. The identified major QTL on C09 and the minor QTL on C07 detected in *B. incana* might support the hypothesis of different resistance mechanisms existing in different wild Brassica species. Our recent data support that the wild Brassica species *B. drepanensis*, *B. rupestris*, and *B. insularis* (data not shown) are valuable genetic sources for breeding for resistance against SSR, which can be partially transferred into the *B. napus* gene pool with MAS as demonstrated by Mei et al. (2015).

Trichome-phenotype is partially co-localized but not associated with Sclerotinia-resistance

Non-glandular trichomes act mainly as physical barriers towards biotic stresses, whereas glandular trichomes can secrete chemicals with antifungal activity (Hauser 2014). It was shown that non-glandular trichomes of *Brassica villosa* subsp. *drepanensis* accumulated high levels of metals (Nayidu et al. 2014a) but their role in plant resistance against Sclerotinia is unknown. The fact that the petiole-assay clearly distinguish resistant and susceptible parental plants implies that trichomes do not play an essential role in plant resistance. Microscopic images suggest that trichomes in *B. villosa* seem to be anchor points for the mycelia on the surface rather than being a barrier to the fungus. In support of this, we did not find a consistent trend between decreasing lesion-sizes and increasing trichome-phenotype with one exception, in which smaller leaf- and petiole-lesions were given in the densely haired trichome-group ‘4’ once. In one petiole-assay, hairy F_2-individuals of trichome-group ‘3’ were to contrast significantly more susceptible to the Sclerotinia infection as compared to the grand mean of all groups. Interestingly, we found that the genetic region of t1QTLb for trichomes was overlapping with that of the major QTL for Sclerotinia-resistance on chromosome C01. Peaks of both QTLs were detected between the markers Bn-scaff_15747_1-p105633 (14,270,425 bp) and Bn-scaff_15747_1-p105633 (16,593,775 bp). It is to mention that the smaller lesion values in the trichome-group ‘4’ co-occurred with l2QTLb2 in Population B, which showed also the strongest correlation between leaf- and petiole-lesions. Thus, we believe that these loci are partially co-segregating but the link is masked by low effect-sizes, such as in the petiole-assay. Following this, we conclude that trichomes are not an essential element contributing to Sclerotinia-resistances in the wild *B. villosa*, though they are partially co-localized on chromosome C01.

Trichome-phenotypes are partially conserved in wild Brassica species

In *A. thaliana*, it has been shown that trichome-morphology is regulated by a complex network of multiple transcription factors, including the positive enhancers GL1, GL2, GL3, EGL3, TTG1, and the negative regulator TRY (Balkunde et al. 2010). Expression analysis of these orthologous genes in the closely related *B. villosa* subsp. *drepanensis* identified three copies of the TRY gene allocated to chromosomes C02, C03, and C09 (Nayidu et al. 2014b). We identified five orthologous genes of TRY from *A. thaliana* (At5g53200) in our RNAseq data, of which one copy (Bo1g051040) is located at 14,433,200 bp on C01 in the *B. oleracea* ‘TO1000’ genome within the t1QTLb peak-marker Bn-scaff_22790_1-p152675 (16,593,775 bp) and the flanking marker Bn-scaff_15747_1-p105633 (14,270,425 bp). The gene was weakly present in *B. oleracea* (FPKM = 0.129) in the inoculated sample. One copy of GL1 (Bo7g090950) and TTG1 (Bo7g096780) are located on chromosome C07 within the physical interval of t5QTLb (27,506,654 bp – 40,491,426 bp). Only TTG1 was present in our RNAseq data and showed no noticeable difference in abundance between both species. We identified two copies of EGL3 (Bo9g029320; Unigene.32857) both located on chromosome C09 out of the physical interval of t3QTLb. No difference in gene expression was observed between the glabrous and the hairy species. Our data suggests that these copies may not be involved in the trichome-phenotype in our *B. villosa* species. Nayidu et al. (2014b) measured a high gene expression of the negative regulator TRY in their wild *B. villosa* species and identified one copy (TRY-1) with higher transcript abundance compared to the other two copies by RNAseq. This is contradictory to the known model in *A. thaliana* in which TRY

inhibits trichome-development (Hülskamp et al. 1994). Further, we did not identifiy any gene expression of the TRY locus in our *B. villosa* species and a very low gene abundance in the glabrous *B. oleracea*. Mei et al. (2017) reported a 3:1 segregation pattern between glabrous and hairy plants in 1063 F_2-plants from their mapping population and identified one major QTL for leaf-trichomes on chromosome C01 with the TRY (Bol013124) gene as major candidate within the QTL. The gene was successfully used as functional cleaved amplified polymorphic site (CAPS) marker for the selection of glabrous and hairy individuals in $F_{2:3}$ families. In contrast, in our study a significant deviation from a 3:1 segregation was given and the alleles from the glabrous *B. oleracea* were dominant in the major QTL on C01. A direct comparison to our study is difficult since Mei et al. (2017) used the *B. oleracea* var. *capitata* reference genome, but a DNA sequence alignment of these two genes revealed noticeable structural differences and it is unclear whether Bol013124 and Bo1g051040 are two distinct genes or allelic variants and if other orthologous genes of TRY, GL1, TTG1, and EGL3 may play an important role in our *B. villosa* species. It is reasonable to assume that the QTL identified by Mei et al. (2017) and our QTL are a conserved locus in the wild Brassica species. The discrepancy between the segregation patterns in these two studies might be caused technically rather than genetically. Further analyses, including the gene expression analysis of the TRY locus and the functional validation of the CAPS marker in our mapping populations may shed more light on molecular mechanisms of trichome-phenotypes observed in *B. villosa* and *B. incana*.

Differential activation of the ET-/JA-activated signaling pathways

Our data shows that ET and ABA were the most addressed phytohormones in response to the Sclerotinia-inoculation. Though a significant response of the ET-activated signaling pathway was detected in both species (BRA1896 = -12.05 $\log_{10}$-FDR; BRA1909 = -5.2 $\log_{10}$-FDR), it was remarkably stronger enriched in the resistant *B. villosa*. We further identified 17 significantly differentially regulated downstream ET response transcription factors (ERF) between *B. villosa* and *B. oleracea* as a result of the Sclerotinia-inoculation. 14 of these ERFs were positively induced in *B. villosa*. These different expression profiles and the increase of expression of the ethylene receptor gene ETR2 in *B. villosa* at 16 hpi support the assumption that the resistant transcriptome response is distinctly regulated through the ET-activated signaling pathway and even increases during pathogenesis in the resistant host. Interestingly, we observed higher gene expression profiles of the JA-biosynthesis markers AOC3 and LOX3 in the susceptible *B. oleracea*, which is in accordance with the RNAseq that showed a stronger significant response to JA in this species. Thus, we also assume a distinct activation of the JA-mediated signaling pathway in the two species. The ET- and JA-mediated signaling pathways are key components in regulating plant defense to necrotrophic pathogens and synergize the ERF branch via ERF1/ORA59 (Pré et al. 2008, Broekgaarden et al. 2015). A key marker gene of the ERF branch is PDF1.2 which is regulated by ORA59, an essential integrator of the ET- and JA-signal transduction pathway (Pré et al. 2008). Our data showed significant expression of one ORA59-like gene (Bo8g114710) in *B. villosa* but no significant induction of PDF1.2. Therefore, we assume that the ET- and JA-signaling pathways are not synergize the common ERF branch and activate different resistance mechanisms in both species. Yang et al. (2017) demonstrated that an infection of resistant rice cultivars with the blast fungus *M. oryzae* activated the ET-signaling pathway resulting in an increase of ROS and phytoalexin production which is in accordance with our observed significant enrichment of the phytoalexin biosynthetic process and a specific response to ROS in the resistant *B. villosa*. Conversely, the susceptible *B. oleracea* showed a strong response of the glucosinolate and sulfur compound metabolic process also observed in *B. napus* in response to Sclerotinia and might be a result of the JA-mediated pathway (Wei et al. 2016). Strikingly, the ABA-activated signaling pathway was specifically addressed in the susceptible *B. oleracea* (BRA1896 = -0.13 $\log_{10}$-FDR; BRA1909 = -1.95 $\log_{10}$-FDR) in which 19 ABA-associated genes showed a significant difference in expression between both species in response to the Sclerotinia-inoculation. The JA-mediated MYC branch, antagonistic to the ERF branch, is responsible for defense against herbivores and co-regulated by ABA (Vos et al. 2015, Broekgaarden et al. 2015). However, the orthologue Bo2g159220 of the MYC-marker gene VSP2 was downregulated in *B. oleracea*. An antagonistic suppression of the JA-activated pathway by SA might be indicated by a higher expression of PR1 in *B. villosa* compared to *B. oleracea*. But a more detailed investigation on the crosstalk of the hormone-mediated signalling pathways is needed as expressions of PR1 and PDF1.2 were vague in both species.

Integrated transcriptome analysis reveals novel *B. villosa*-specific genes

The identification of promising candidates from the QTL is limited to genes that are present in the 'TO1000' reference genome. An analysis of the reference genes in the peak regions of chromosome C01 and C07 revealed 242 and 27 genes, respectively. Gene expression profiles showed subtle differences further impeding the selection of candidates. We hypothesized that important *B. villosa*-specific genes are absent in the 'TO1000' reference genome and performed an integrated reference- and *de novo*-based

RNAseq analysis. Hence, we were able to identify 413 upregulated *B. villosa*-specific genes in response to the Sclerotinia-inoculation. By a comparative functional analysis, 58 candidate genes were identified that are associated with a defense response but are lacking a genetic link to the here identified QTLs. Genomic re-sequencing of *B. villosa* may facilitate a linkage of these genes to the QTLs and allow the selection of promising candidates for further studies.

Conclusion

Our study shows that the wild accession *B. villosa* is a novel and unique source of quantitative resistance against the economically important fungal pathogen *S. sclerotiorum*. We identified genomic regions in *B. villosa* that will be useful in breeding for improved Sclerotinia-resistance and showed that the genetic basis may only be partially conserved across wild Brassica species. Furthermore, we show that the ET-activated signaling pathway is an essential regulator of the defense response of the resistant *B. villosa* and associated with an activation of the phytoalexin biosynthetic process and a response to ROS. We point out that the wild *Brassica oleracea* complex is an important source for resistance breeding in oilseed rape against Sclerotinia. We demonstrated the successful application of the *B. napus* 15k-SNP-chip-microarray for genetic mapping in the wild *B. villosa* and propose that a similar strategy in other wild Brassica species with high resistance against Sclerotinia, such as *B. drepanensis* or *B. rupestris*, will reveal more QTLs. Furthermore, we think that a similar approach in the *Brassica rapa* complex may result in the identification of improved resistance in the highly susceptible A-genome (Mei et al. 2011). We conclude that trichomes are non-functional in defense against *S. sclerotiorum* in the wild *B. villosa* but are partially co-localized with Sclerotinia-resistance.

Declarations

Acknowledgements

We gratefully thank Dr. Plieske from TraitGenetics for the helpful support, Prof. Dr. Broman for the helpful advices with R/qtl, Annalena Hartmann and Martina Wittke for the excellent technical assistance. The authors thank the Stiftung Schleswig-Holsteinische Landschaft for providing scholarship to Thomas Bergmann (2018/06), and DAAD and BLE for travel grants (Grant no. 57317839, 13/14-15-CHN).

Funding

This work was financially supported by the Bundesministerium für Bildung und Forschung (BMBF, Grant no. 0315637 B), the Bundesministerium für Ernährung und Landwirtschaft (BMEL) and the Fachagentur für Nachwachsende Rohstoffe (Grant no. 22410312, FKZ22006516).

Competing interests

The authors declare that they have no conflict of interest.

Ethics approval

Not applicable.

Consent to participate

Not applicable.

Consent for publication

Not applicable.

Availability of data and material

The main data is provided in the electronic supplementary material. Additional data is available on request. Raw sequencing data is deposited in the National Center for Biotechnology Information (https://www.ncbi.nlm.nih.gov/bioproject) with the following BioProject-ID: PRJNA706136.

Code availability

The main code and results are available as reports at http://doi.org/10.5281/zenodo.4556803.

Contributions

TB conducted main experiments and constructed the genetic map, designed and conducted the RNAseq, qPCR experiments, and bioinformatics analyses, and drafted the manuscript. JM contributed to generation of population, phenotyping and genotyping experiments. MS supported phenotyping and computational analysis. WY supported generation of population, phenotyping and genotyping experiments. MH supported the statistical analysis. SR and GL provided plant materials and supported the project. DG conceived and directed the project and finalized the manuscript. All authors read and approved the final manuscript.

References

Altschul SF, Gish W, Miller W, Myers EW, Lipman DJ (1990) Basic local alignment search tool. Journal of Molecular Biology 215(3):403–410. doi: 10.1016/S0022-2836(05)80360-2

Amselem J, Cuomo CA, van Kan JAL, Viaud M, Benito EP, Couloux A, Coutinho PM, Vries RP de, Dyer PS, Fillinger S, Fournier E, Gout L, Hahn M, Kohn L, Lapalu N, Plummer KM, Pradier J-M, Quévillon E, Sharon A, Simon A, Have A ten, Tudzynski B, Tudzynski P, Wincker P, Andrew M, Anthouard V, Beever RE, Beffa R, Benoit I, Bouzid O, Brault B, Chen Z, Choquer M, Collémare J, Cotton P, Danchin EG, Da Silva C, Gautier A, Giraud C, Giraud T, Gonzalez C, Grossetete S, Güldener U, Henrissat B, Howlett BJ, Kodira C, Kretschmer M, Lappartient A, Leroch M, Levis C, Mauceli E, Neuvéglise C, Oeser B, Pearson M, Poulain J, Poussereau N, Quesneville H, Rascle C, Schumacher J, Ségurens B, Sexton A, Silva E, Sirven C, Soanes DM, Talbot NJ, Templeton M, Yandava C, Yarden O, Zeng Q, Rollins JA, Lebrun M-H, Dickman M (2011) Genomic analysis of the necrotrophic fungal pathogens Sclerotinia sclerotiorum and Botrytis cinerea. PLoS genetics 7(8):e1002230. doi: 10.1371/journal.pgen.1002230

Balkunde R, Pesch M, Hülskamp M (2010) Trichome Patterning in Arabidopsis thaliana. In: Plant Development, vol 91. Elsevier, pp 299–321

Behla R, Hirani AH, Zelmer CD, Yu F, Fernando WGD, McVetty P, Li G (2017) Identification of common QTL for resistance to Sclerotinia sclerotiorum in three doubled haploid populations of Brassica napus (L.). Euphytica 213(11):88. doi: 10.1007/s10681-017-2047-5

Benjamini Y, Hochberg Y (1995) Controlling the False Discovery Rate. A Practical and Powerful Approach to Multiple Testing. Journal of the Royal Statistical Society: Series B (Methodological) 57(1):289–300. doi: 10.1111/j.2517-6161.1995.tb02031.x

Boland GJ, Hall R (1994) Index of plant hosts of Sclerotinia sclerotiorum. Canadian Journal of Plant Pathology 16(2):93–108. doi: 10.1080/07060669409500766

Bolger AM, Lohse M, Usadel B (2014) Trimmomatic. A flexible trimmer for Illumina sequence data. Bioinformatics (Oxford, England) 30(15):2114–2120. doi: 10.1093/bioinformatics/btu170

Bolser D, Staines DM, Pritchard E, Kersey P (2016) Ensembl Plants. Integrating Tools for Visualizing, Mining, and Analyzing Plant Genomics Data. Methods in molecular biology (Clifton, N.J.) 1374:115–140. doi: 10.1007/978-1-4939-3167-5_6

Bolton MD, Thomma BPHJ, Nelson BD (2006) Sclerotinia sclerotiorum (Lib.) de Bary. Biology and molecular traits of a cosmopolitan pathogen. Molecular plant pathology 7(1):1–16. doi: 10.1111/j.1364-3703.2005.00316.x

Broekgaarden C, Caarls L, Vos IA, Pieterse CMJ, van Wees SCM (2015) Ethylene. Traffic Controller on Hormonal Crossroads to Defense. Plant physiology 169(4):2371–2379. doi: 10.1104/pp.15.01020

Broman KW, Sen S (2009) A Guide to QTL Mapping with R/qtl. Statistics for Biology and Health. Springer-Verlag New York, New York, NY

Broman KW, Wu H, Sen S, Churchill GA (2003) R/qtl. QTL mapping in experimental crosses. Bioinformatics (Oxford, England) 19(7):889–890. doi: 10.1093/bioinformatics/btg112

Camacho C, Coulouris G, Avagyan V, Ma N, Papadopoulos J, Bealer K, Madden TL (2009) BLAST+. Architecture and applications. BMC bioinformatics 10:421. doi: 10.1186/1471-2105-10-421

Chen H-F, Wang H, Li Z-Y (2007) Production and genetic analysis of partial hybrids in intertribal crosses between Brassica species (B. rapa, B. napus) and Capsella bursa-pastoris. Plant cell reports 26(10):1791–1800. doi: 10.1007/s00299-007-0392-x

Derbyshire M, Denton-Giles M, Hegedus D, Seifbarghy S, Rollins J, van Kan J, Seidl MF, Faino L, Mbengue M, Navaud O, Raffaele S, Hammond-Kosack K, Heard S, Oliver R (2017) The complete genome sequence of the phytopathogenic fungus Sclerotinia sclerotiorum reveals insights into the genome architecture of broad host range pathogens. Genome biology and evolution. doi: 10.1093/gbe/evx030

Derbyshire MC, Denton-Giles M (2016) The control of sclerotinia stem rot on oilseed rape (Brassica napus). Current practices and future opportunities. Plant Pathol 65(6):859–877. doi: 10.1111/ppa.12517

Ding Y, Mei J, Chai Y, Yu Y, Shao C, Wu Q, Disi JO, Li Y, Wan H, Qian W (2019b) Simultaneous Transcriptome Analysis of Host and Pathogen Highlights the Interaction Between Brassica oleracea and Sclerotinia sclerotiorum. Phytopathology 109(4):542–550. doi: 10.1094/PHYTO-06-18-0204-R

Ding Y, Mei J, Wu Q, Xiong Z, Li Y, Shao C, Wang L, Qian W (2019a) Synchronous improvement of subgenomes in allopolyploid. A case of Sclerotinia resistance improvement in Brassica napus. Mol Breeding 39(1):1. doi: 10.1007/s11032-018-0915-x

El-Gebali S, Mistry J, Bateman A, Eddy SR, Luciani A, Potter SC, Qureshi M, Richardson LJ, Salazar GA, Smart A, Sonnhammer ELL, Hirsh L, Paladin L, Piovesan D, Tosatto SCE, Finn RD (2019) The Pfam protein families database in 2019. Nucleic acids research 47(D1):D427-D432. doi: 10.1093/nar/gky995

Fernández-Bautista N, Domínguez-Núñez J, Moreno MM, Berrocal-Lobo M (2016) Plant Tissue Trypan Blue Staining During Phytopathogen Infection. BIO-PROTOCOL 6(24). doi: 10.21769/BioProtoc.2078

Garg H, Atri C, Sandhu PS, Kaur B, Renton M, Banga SK, Singh H, Singh C, Barbetti MJ, Banga SS (2010) High level of resistance to Sclerotinia sclerotiorum in introgression lines derived from hybridization between wild crucifers and the crop Brassica species B. napus and B. juncea. Field Crops Research 117(1):51–58. doi: 10.1016/j.fcr.2010.01.013

Grabherr MG, Haas BJ, Yassour M, Levin JZ, Thompson DA, Amit I, Adiconis X, Fan L, Raychowdhury R, Zeng Q, Chen Z, Mauceli E, Hacohen N, Gnirke A, Rhind N, Di Palma F, Birren BW, Nusbaum C, Lindblad-Toh K, Friedman N, Regev A (2011) Full-length transcriptome assembly from RNA-Seq data without a reference genome. Nature biotechnology 29(7):644–652. doi: 10.1038/nbt.1883

Gu Z, Eils R, Schlesner M (2016) Complex heatmaps reveal patterns and correlations in multidimensional genomic data. Bioinformatics (Oxford, England) 32(18):2847–2849. doi: 10.1093/bioinformatics/btw313

Gyawali S, Harrington M, Durkin J, Horner K, Parkin IAP, Hegedus DD, Bekkaoui D, Buchwaldt L (2016) Microsatellite markers used for genome-wide association mapping of partial resistance to Sclerotinia sclerotiorum in a world collection of Brassica napus. Mol Breeding 36:72. doi: 10.1007/s11032-016-0496-5

Hauser M-T (2014) Molecular basis of natural variation and environmental control of trichome patterning. Frontiers in plant science 5:320. doi: 10.3389/fpls.2014.00320

Hothorn T, Bretz F, Westfall P (2008) Simultaneous inference in general parametric models. Biometrical journal. Biometrische Zeitschrift 50(3):346–363. doi: 10.1002/bimj.200810425

Hülskamp M, Miséra S, Jürgens G (1994) Genetic dissection of trichome cell development in Arabidopsis. Cell 76(3):555–566. doi: 10.1016/0092-8674(94)90118-x

Joshi RK, Megha S, Rahman MH, Basu U, Kav NNV (2016) A global study of transcriptome dynamics in canola (Brassica napus L.) responsive to Sclerotinia sclerotiorum infection using RNA-Seq. Gene 590(1):57–67. doi: 10.1016/j.gene.2016.06.003

Kim D, Paggi JM, Park C, Bennett C, Salzberg SL (2019) Graph-based genome alignment and genotyping with HISAT2 and HISAT-genotype. Nature biotechnology 37(8):907–915. doi: 10.1038/s41587-019-0201-4

Li B, Dewey CN (2011) RSEM. Accurate transcript quantification from RNA-Seq data with or without a reference genome. BMC bioinformatics 12:323. doi: 10.1186/1471-2105-12-323

Li H, Handsaker B, Wysoker A, Fennell T, Ruan J, Homer N, Marth G, Abecasis G, Durbin R (2009) The Sequence Alignment/Map format and SAMtools. Bioinformatics (Oxford, England) 25(16):2078–2079. doi: 10.1093/bioinformatics/btp352

Li J, Zhao Z, Hayward A, Cheng H, Fu D (2015) Integration analysis of quantitative trait loci for resistance to Sclerotinia sclerotiorum in Brassica napus. Euphytica 205(2):483–489. doi: 10.1007/s10681-015-1417-0

Love MI, Huber W, Anders S (2014) Moderated estimation of fold change and dispersion for RNA-seq data with DESeq2. Genome biology 15(12):550. doi: 10.1186/s13059-014-0550-8

Mei J, Ding Y, Lu K, Wei D, Liu Y, Disi JO, Li J, Liu L, Liu S, McKay J, Qian W (2013) Identification of genomic regions involved in resistance against Sclerotinia sclerotiorum from wild Brassica oleracea. TAG. Theoretical and applied genetics. Theoretische und angewandte Genetik 126(2):549–556. doi: 10.1007/s00122-012-2000-x

Mei J, Liu Y, Wei D, Wittkop B, Ding Y, Li Q, Li J, Wan H, Li Z, Ge X, Frauen M, Snowdon RJ, Qian W, Friedt W (2015) Transfer of sclerotinia resistance from wild relative of Brassica oleracea into Brassica napus using a hexaploidy step. TAG. Theoretical and applied genetics. Theoretische und angewandte Genetik 128(4):639–644. doi: 10.1007/s00122-015-2459-3

Mei J, Qian L, Disi JO, Yang X, Li Q, Li J, Frauen M, Cai D, Qian W (2011) Identification of resistant sources against Sclerotinia sclerotiorum in Brassica species with emphasis on B. oleracea. Euphytica 177(3):393–399. doi: 10.1007/s10681-010-0274-0

Mei J, Shao C, Yang R, Feng Y, Gao Y, Ding Y, Li J, Qian W (2020) Introgression and pyramiding of genetic loci from wild Brassica oleracea into B. napus for improving Sclerotinia resistance of rapeseed. TAG. Theoretical and applied genetics. Theoretische und angewandte Genetik 133(4):1313–1319. doi: 10.1007/s00122-020-03552-w

Mei J, Wang J, Li Y, Tian S, Wei D, Shao C, Si J, Xiong Q, Li J, Qian W (2017) Mapping of genetic locus for leaf trichome in Brassica oleracea. TAG. Theoretical and applied genetics. Theoretische und angewandte Genetik 130(9):1953–1959. doi: 10.1007/s00122-017-2936-y

Nayidu NK, Kagale S, Taheri A, Withana-Gamage TS, Parkin IAP, Sharpe AG, Gruber MY, Schiefelbein J (2014b) Comparison of Five Major Trichome Regulatory Genes in Brassica villosa with Orthologues within the Brassicaceae. PloS one 9(4):e95877. doi: 10.1371/journal.pone.0095877

Nayidu NK, Tan Y, Taheri A, Li X, Bjorndahl TC, Nowak J, Wishart DS, Hegedus D, Gruber MY (2014a) Brassica villosa, a system for studying non-glandular trichomes and genes in the Brassicas. Plant molecular biology 85(4-5):519–539. doi: 10.1007/s11103-014-0201-1

Parkin IAP, Koh C, Tang H, Robinson SJ, Kagale S, Clarke WE, Town CD, Nixon J, Krishnakumar V, Bidwell SL, Denoeud F, Belcram H, Links MG, Just J, Clarke C, Bender T, Huebert T, Mason AS, Pires JC, Barker G, Moore J, Walley PG, Manoli S, Batley J, Edwards D, Nelson MN, Wang X, Paterson AH, King G, Bancroft I, Chalhoub B, Sharpe AG (2014) Transcriptome and methylome profiling reveals relics of genome dominance in the mesopolyploid Brassica oleracea. Genome biology 15(6):R77. doi: 10.1186/gb-2014-15-6-r77

Pertea G, Pertea M (2020) GFF Utilities. GffRead and GffCompare. F1000Research 9. doi: 10.12688/f1000research.23297.2

Pertea M, Kim D, Pertea GM, Leek JT, Salzberg SL (2016) Transcript-level expression analysis of RNA-seq experiments with HISAT, StringTie and Ballgown. Nature protocols 11(9):1650–1667. doi: 10.1038/nprot.2016.095

Pertea M, Pertea GM, Antonescu CM, Chang T-C, Mendell JT, Salzberg SL (2015) StringTie enables improved reconstruction of a transcriptome from RNA-seq reads. Nature biotechnology 33(3):290–295. doi: 10.1038/nbt.3122

Pfaffl MW (2001) A new mathematical model for relative quantification in real-time RT-PCR. Nucleic acids research 29(9):e45. doi: 10.1093/nar/29.9.e45

Pinheiro J, Bates D, DebRoy S, Sarkar D (2020) nlme. Linear and nonlinear mixed effects models. https://CRAN.R-project.org/package=nlme

Pré M, Atallah M, Champion A, Vos M de, Pieterse CMJ, Memelink J (2008) The AP2/ERF domain transcription factor ORA59 integrates jasmonic acid and ethylene signals in plant defense. Plant physiology 147(3):1347–1357. doi: 10.1104/pp.108.117523

Quinlan AR, Hall IM (2010) BEDTools. A flexible suite of utilities for comparing genomic features. Bioinformatics (Oxford, England) 26(6):841–842. doi: 10.1093/bioinformatics/btq033

R Core Team (2019) R: A language and environment for statistical computing, Vienna, Austria

Rogers SO, Bendich AJ (1985) Extraction of DNA from milligram amounts of fresh, herbarium and mummified plant tissues. Plant molecular biology 5(2):69–76. doi: 10.1007/BF00020088

Taylor A, Coventry E, Jones JE, Clarkson JP (2015) Resistance to a highly aggressive isolate of Sclerotinia sclerotiorum in a Brassica napus diversity set. Plant Pathol 64(4):932–940. doi: 10.1111/ppa.12327

Taylor A, Rana K, Handy C, Clarkson JP (2018) Resistance to Sclerotinia sclerotiorum in wild Brassica species and the importance of Sclerotinia subarctica as a Brassica pathogen. Plant Pathol 67(2):433–444. doi: 10.1111/ppa.12745

The Uniprot Consortium (2019) UniProt. A worldwide hub of protein knowledge. Nucleic acids research 47(D1):D506-D515. doi: 10.1093/nar/gky1049

Uloth MB, You MP, Finnegan PM, Banga SS, Banga SK, Sandhu PS, Yi H, Salisbury PA, Barbetti MJ (2013) New sources of resistance to Sclerotinia sclerotiorum for crucifer crops. Field Crops Research 154:40–52. doi: 10.1016/j.fcr.2013.07.013

Vos IA, Moritz L, Pieterse CMJ, van Wees SCM (2015) Impact of hormonal crosstalk on plant resistance and fitness under multi-attacker conditions. Front. Plant Sci. 6:639. doi: 10.3389/fpls.2015.00639

Wang H, Liu G, Zheng Y, Wang X, Yang Q (2004) Breeding of the Brassica napus cultivar Zhongshuang 9 with high-resistance to Sclerotinia sclerotiorum and dynamics of its important defense enzyme activity. Scientia Agriculutra Sinica 37:23–28

Wang Y, Hou Y-P, Chen C-J, Zhou M-G (2014) Detection of resistance in Sclerotinia sclerotiorum to carbendazim and dimethachlon in Jiangsu Province of China. Australasian Plant Pathol. 43(3):307–312. doi: 10.1007/s13313-014-0271-1

Wei D, Mei J, Fu Y, Disi JO, Li J, Qian W (2014) Quantitative trait loci analyses for resistance to Sclerotinia sclerotiorum and flowering time in Brassica napus. Mol Breeding 34(4):1797–1804. doi: 10.1007/s11032-014-0139-7

Wei L, Jian H, Lu K, Filardo F, Yin N, Liu L, Qu C, Li W, Du H, Li J (2016) Genome-wide association analysis and differential expression analysis of resistance to Sclerotinia stem rot in Brassica napus. Plant biotechnology journal 14(6):1368–1380. doi: 10.1111/pbi.12501

Wickham H (2016) ggplot2. Elegant graphics for data analysis. Use R! Springer, Cham

Wickham H, François R, Henry L, Müller K (2019) dplyr. A Grammar of Data Manipulation. https://CRAN.R-project.org/package=dplyr

Wu J, Cai G, Tu J, Li L, Liu S, Luo X, Zhou L, Fan C, Zhou Y (2013) Identification of QTLs for resistance to sclerotinia stem rot and BnaC.IGMT5.a as a candidate gene of the major resistant QTL SRC6 in Brassica napus. PloS one 8(7):e67740. doi: 10.1371/journal.pone.0067740

Wu J, Zhao Q, Liu S, Shahid M, Lan L, Cai G, Zhang C, Fan C, Wang Y, Zhou Y (2016) Genome-wide Association Study Identifies New Loci for Resistance to Sclerotinia Stem Rot in Brassica napus. Frontiers in plant science 7:1418. doi: 10.3389/fpls.2016.01418

Xie C, Mao X, Huang J, Ding Y, Wu J, Dong S, Kong L, Gao G, Li C-Y, Wei L (2011) KOBAS 2.0. A web server for annotation and identification of enriched pathways and diseases. Nucleic acids research 39(Web Server issue):W316-22. doi: 10.1093/nar/gkr483

Yin X, Yi B, Chen W, Zhang W, Tu J, Fernando WGD, Fu T (2010) Mapping of QTLs detected in a Brassica napus DH population for resistance to Sclerotinia sclerotiorum in multiple environments. Euphytica 173(1):25–35. doi: 10.1007/s10681-009-0095-1

You MP, Uloth MB, Li XX, Banga SS, Banga SK, Barbetti MJ (2016) Valuable New Resistances Ensure Improved Management of Sclerotinia Stem Rot (Sclerotinia sclerotiorum) in Horticultural and Oilseed Brassica Species. J Phytopathol 164(5):291–299. doi: 10.1111/jph.12456

Young MD, Wakefield MJ, Smyth GK, Oshlack A (2010) Gene ontology analysis for RNA-seq. Accounting for selection bias. Genome biology 11(2):R14. doi: 10.1186/gb-2010-11-2-r14

Zhao J, Meng J (2003) Genetic analysis of loci associated with partial resistance to Sclerotinia sclerotiorum in rapeseed (Brassica napus L.). TAG. Theoretical and applied genetics. Theoretische und angewandte Genetik 106(4):759–764. doi: 10.1007/s00122-002-1171-2

Zhao J, Peltier AJ, Meng J, Osborn TC, Grau CR (2004) Evaluation of Sclerotinia Stem Rot Resistance in Oilseed Brassica napus Using a Petiole Inoculation Technique Under Greenhouse Conditions. Plant disease 88(9):1033–1039. doi: 10.1094/PDIS.2004.88.9.1033

Zhao J, Udall JA, Quijada PA, Grau CR, Meng J, Osborn TC (2006) Quantitative trait loci for resistance to Sclerotinia sclerotiorum and its association with a homeologous non-reciprocal transposition in Brassica napus L. TAG. Theoretical and applied genetics. Theoretische und angewandte Genetik 112(3):509–516. doi: 10.1007/s00122-005-0154-5

Zhou F, Zhang X-L, Li J-L, Zhu F-X (2014) Dimethachlon Resistance in Sclerotinia sclerotiorum in China. Plant disease 98(9):1221–1226. doi: 10.1094/PDIS-10-13-1072-RE

Tables

Table 1 Identified QTLs for Sclerotinia-resistance and trichome-phenotype in the mapping populations.

Trait	QTL	LOD	LG	Position [cM]	Peak-Marker[a]	P-value	Bayes interval[b]		Var %	Add[c]	Dom[d]
							[cM]	[Mbp]			
Sclerotinia-resistance	pQTLa	6.23	C01	53	Bn-scaff_19564_1-p17934	< 0.001	11.61	24.2	15.8	3.82	-0.62
	l2QTLb	6.16	C01	51	Bn-scaff_22790_1-p152675	< 0.001	20	28.6	16.5	123.92	88.16
	l3QTLb	4.07	C07	79.6	Bn-scaff_16110_1-p976517	0.018	9.16	1.5	10.4	15.92	-90.28
	p1QTLb1	3.79	C03	12	Bn-scaff_18936_1-p269153	0.032	18.05	4.2	8.1	2.01	1.25
	p1QTLb2	4.56	C07	54.3	Bn-scaff_16069_1-p4306874	< 0.01	13.14	2	9.9	2.35	1.05
	p3QTLb1*	3.22	C03	13.1	Bn-scaff_18936_1-p269153	0.087	96.16	50.2	3.9	1.5	-0.5
	p3QTLb2*	3.78	C07	46.9	Bn-scaff_16069_1-p2611780	0.031	32.41	5.8	4.8	1.3	1.5
Merged	pAlB2	10.7	C01	50	Bn-scaff_15747_1-p105633	0	7.15	16	14.2	0.37	0.15
	pAlB3	3.73	C07	80.5	Bn-scaff_16110_1-p426547	0.035	16.7	2.3	4.9	0.17	-0.18
	pApB1	5.29	C07	58	Bn-scaff_16069_1-p4828119	< 0.01	8.8	1.4	7.8	0.29	0.001
	pApB3	4.41	C07	59	Bn-scaff_16110_1-p3674923	0.01	33.75	5.6	5.2	0.23	0.03
Trichomes	t1QTLb	23.04	C01	50	Bn-scaff_15747_1-p105633	0	5.76	3.6	36.8	-1.51	-0.6
	t2QTLb	3.83	C04b	8.18	Bn-scaff_16888_1-p1168071	0.035	20.18	3.1	5.5	-0.53	0.12
	t3QTLb	8.49	C09	7	Bn-scaff_17526_1-p1667260	0	6	1.2	12.9	-0.85	0.006
	t4QTLb	3.58	C03	52	Bn-scaff_16352_1-p1063388	0.058	35.46	14.7	3.9	-0.45	0.25
	t5QTLb	5.96	C07	33	Bn-A06-p24207308	< 0.001	13.5	12.9	5.6	-0.51	-0.12

QTL were labeled by trait ('p' = petiole, 'l' = leaf, and 't' = trichomes) with numbers representing the replication, by mapping population ('a' = Population A, 'b' = Population B) followed by a second number to distinguish multiple QTL from one assay. Merged QTL were labeled by trait and mapping population (in capitals) and numbers representing the replication of the assay.

[a] Marker at peak or nearest to the peak.

[b] Estimated QTL-interval via the Bayes credible method in cM and in Mbp

[c] Additive effect. Positive values indicate alleles from the susceptible parent (BRA1909) increase lesion values and decrease the trichome-phenotype.

[d] Dominant effect. Positive values for lesion size and negative values for the trichome-phenotype indicate alleles from the susceptible parent (BRA1909) are dominant.

*Identified via a non-parametric model: interval, variance, additive, and dominance effects are calculated via Haley-Knott and may be underestimated.

Supplementary Files

Data S1 Phenotypes of Population A including parental plants (A1909/A1896)

Data S2 Phenotypes of Population B including parental plants (B1909/B1896) and 'Falcon'

Data S3 Individual phenotypes of parental plants in both populations

Data S4 Genetic and physical map

Data S5 Mapping data for QTL-analysis in R/qtl

Data S6 Primer for qPCR-analysis

Data S7 Biological processes enrichment data

Data S8 Molecular function enrichment data

Data S9 Cellular component enrichment data

Data S10 Candidate genes in pAlB2

Data S11 Candidate genes in pApB1/pApB3

Data S12 *B. villosa*-specifically upregulated defense-related DEGs

Supplementary figure and table legends

Fig. S1 Detached leaf- and petiole-assay. **A** Leaf- (top) and petiole- (bottom) lesions of the susceptible B. oleracea (BRA1909). **B** Leaf- (top) and petiole- (bottom) lesions of the resistant B. villosa (BRA1896). Leaves and petioles were infected with PDA-plugs of actively growing Sclerotinia-mycelia attached to the leaf surface and the open cut of the petiole. Mock-plugs (red circle) were used as controls. **C-D** Phenotypical comparison of the parental accessions in the two mapping populations via the detached **C** leaf- and **D** petiole-assay at 2 dpi under greenhouse conditions. **p-value < 0.01; ***p-value < 0.001.

Fig. S2 Trypan blue staining of infected leaves of **A-B** BRA1909 and **C-D** BRA1896. Mycelia and dead plant cells are stained with Trypan blue. In the susceptible accession BRA1909, the fungal tends to a dense and compact structured growth mainly within the necrotic tissue with a delimited junction between healthy and infected tissue indicated by a layer of dead plant cells in front of the hyphae. In the resistant BRA1896, fungal expansion appears less structured, focusing mainly on the leaf surface with no delimited junction between healthy and infected tissue.

Fig. S3 Venn diagram showing the proportion of F_2-individuals from both mapping populations that are commonly classified as ‘resistant’, ‘intermediate’, and ‘susceptible’ in the leaf- and the petiole-assay. The grouping is based on the comparison to the resistant (BRA1896) and the susceptible (BRA1909) parents.

Fig. S4 LOD-profiles for **A** leaf- and **B** petiole-assays in Population A (red) and Population B (dark gray = 1st assay; turquoise = 2nd assay; blue = 3rd assay). Horizontal lines indicate LOD-thresholds. QTLs are labeled and marked by black dots.

Fig. S5 Sample distance matrix (**A**) and principal component analysis (PCA, **B**) of RNAseq samples after regularized log-transformation. PC1: variance caused by the species; PC2: variance caused by the Sclerotinia-inoculation. BRA1909 = B. oleracea, BRA1896 = B. villosa;
C = Mock, I = Inoculated.

Fig. S6 Marker gene expression analysis by real-time quantitative PCR at 8 hpi and 16 hpi with Sclerotinia in the resistant B. villosa (BRA1896) and the susceptible B. oleracea (BRA1909). Asterisks indicate a significant expression compared to the control group. **p-value < 0.01; ***p-value < 0.001.

Fig. S7 Marker gene expression comparison of qPCR and RNAseq data at 8 hpi. Asterisks indicate a significant expression compared to the control group. BRA1896 = B. villosa; BRA1909 = B. oleracea. Note: the expression of PDF1.2 in B. oleracea in the RNAseq is based on an abundance of < 0.1 FPKM in both the control and the inoculated samples and absent in B. villosa. qPCR expression was log2-transformed for better comparison.

Table S1 Statistics of the genetic map.

Figures

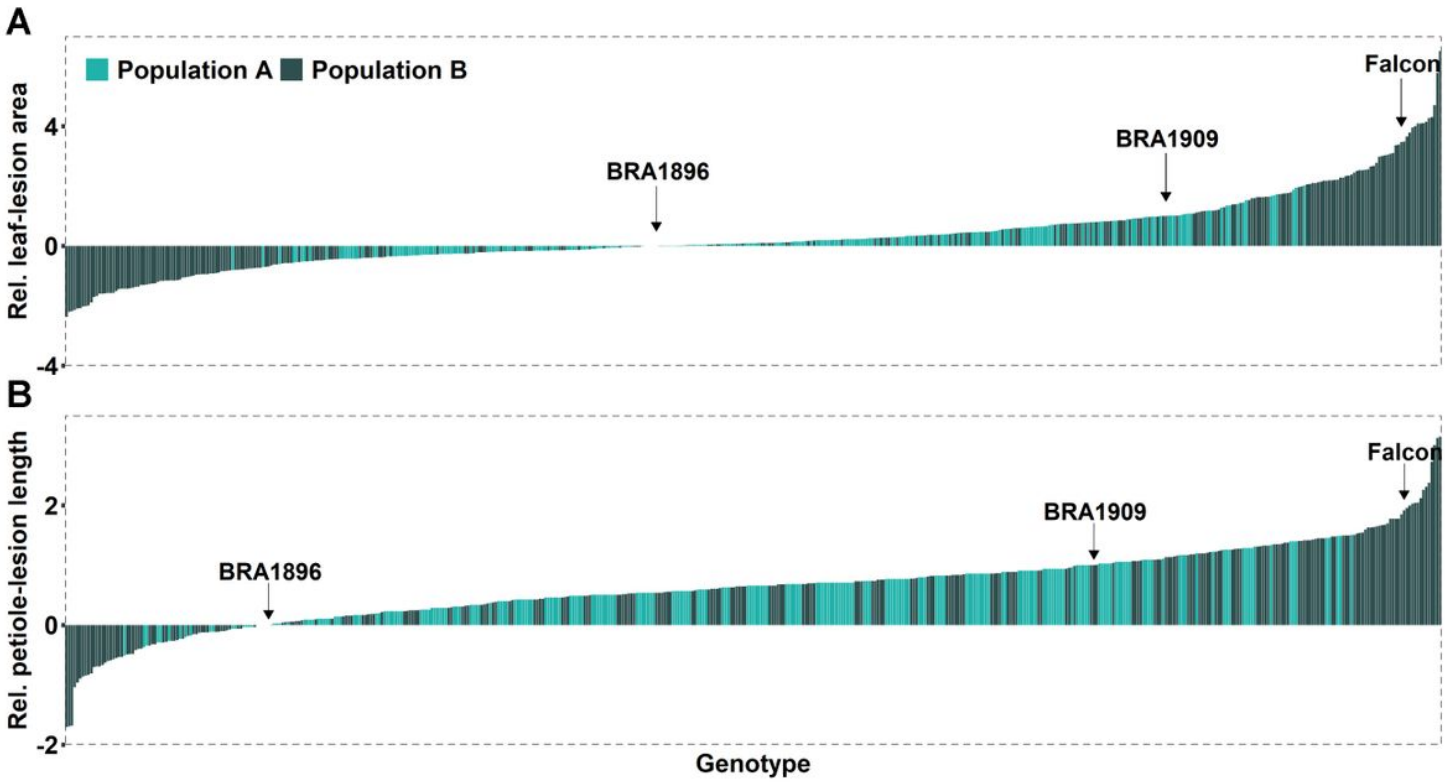

Figure 1

Relative lesion size distribution in both populations. A Relative leaf-lesion area distribution. B Relative petiole-lesion length distribution. (Light green) Lesion values of Population A. (Dark gray) Lesion values of Population B. Relative values < 0 mean more resistant compared to B. villosa (BRA1896), relative values > 1 mean more susceptible compared to B. oleracea (BRA1909), and relative values between 0 and 1 represent the category of 'intermediate'. Positions of B. villosa, B. oleracea, and B. napus (Falco') are indicated by arrows.

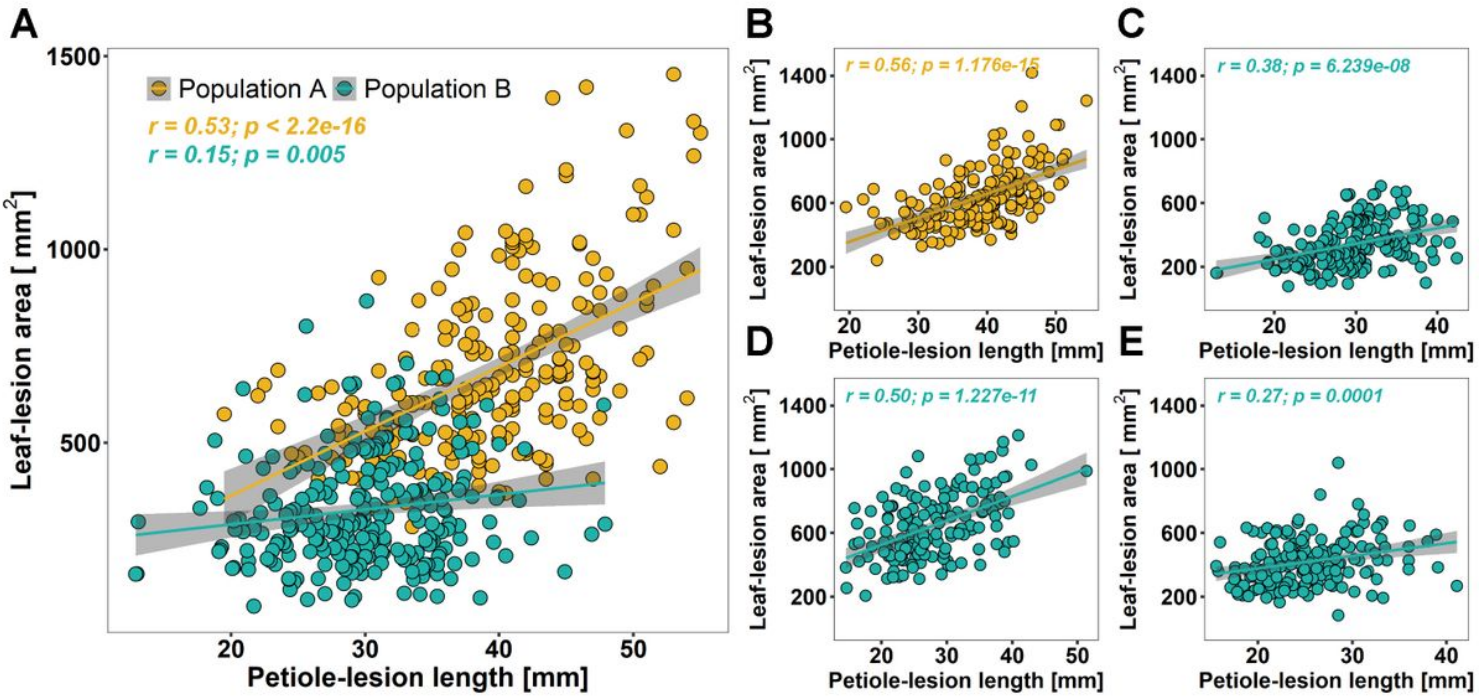

Figure 2

Scatterplot of leaf- and petiole-lesions. A Lesion values of all individuals in Population A (yellow) and Population B (cyan). B Lesion values of all genotyped individuals in Population A. C-D Lesion values of all genotyped individuals in Population B in all three replications. C 1st assay, D 2nd assay, E 3rd assay. r = coefficient of correlation.

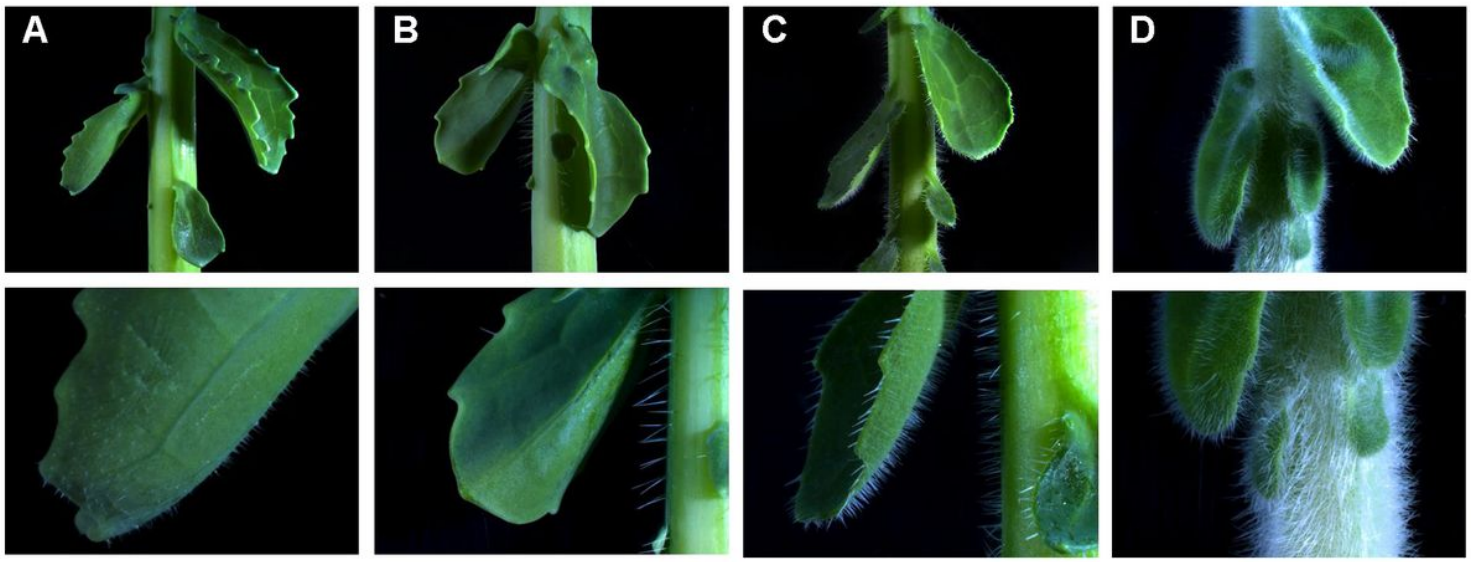

Figure 3

Exemplary illustration of the observed trichome variation in F2-individuals in Population B. A-C The hairiness ranged from glabrous and slightly haired to densely haired individuals. D Trichome-phenotype of the highly resistant B. villosa (BRA1896).

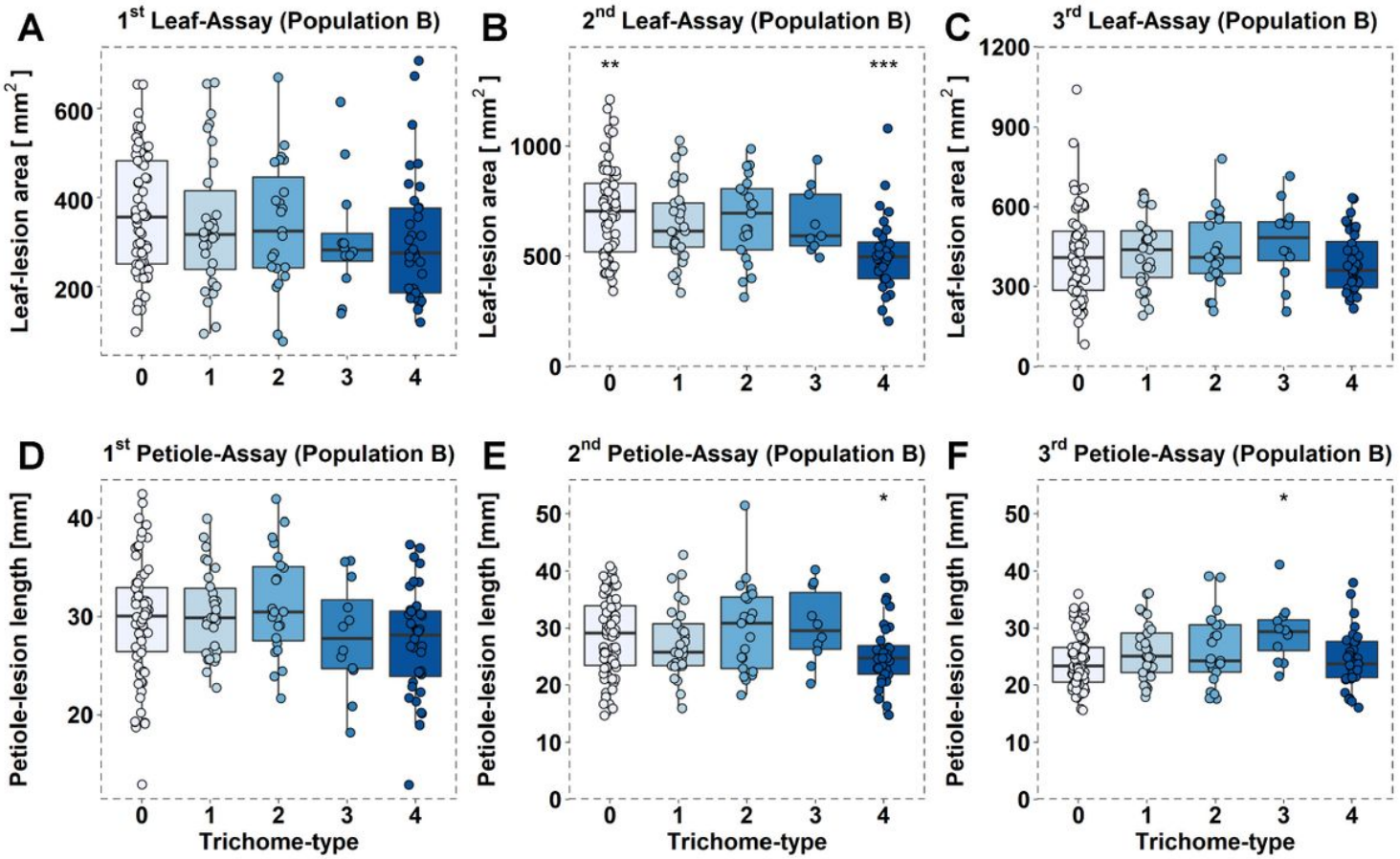

Figure 4

Comparison of trichome-groups in Population B with regard to their leaf- and petiole-lesion sizes across all replications. A-C Leaf-lesion areas and D-F petiole-lesion lengths of the trichome-groups from the 1st to the 3rd replication. Groups were compared by a one-way ANOVA and compared to the grand mean of all groups. *p < 0.05; **p < 0.01; ***p < 0.001. Trichome-types are presented in increments from 0 (glaborus) to 4 (densely haired).

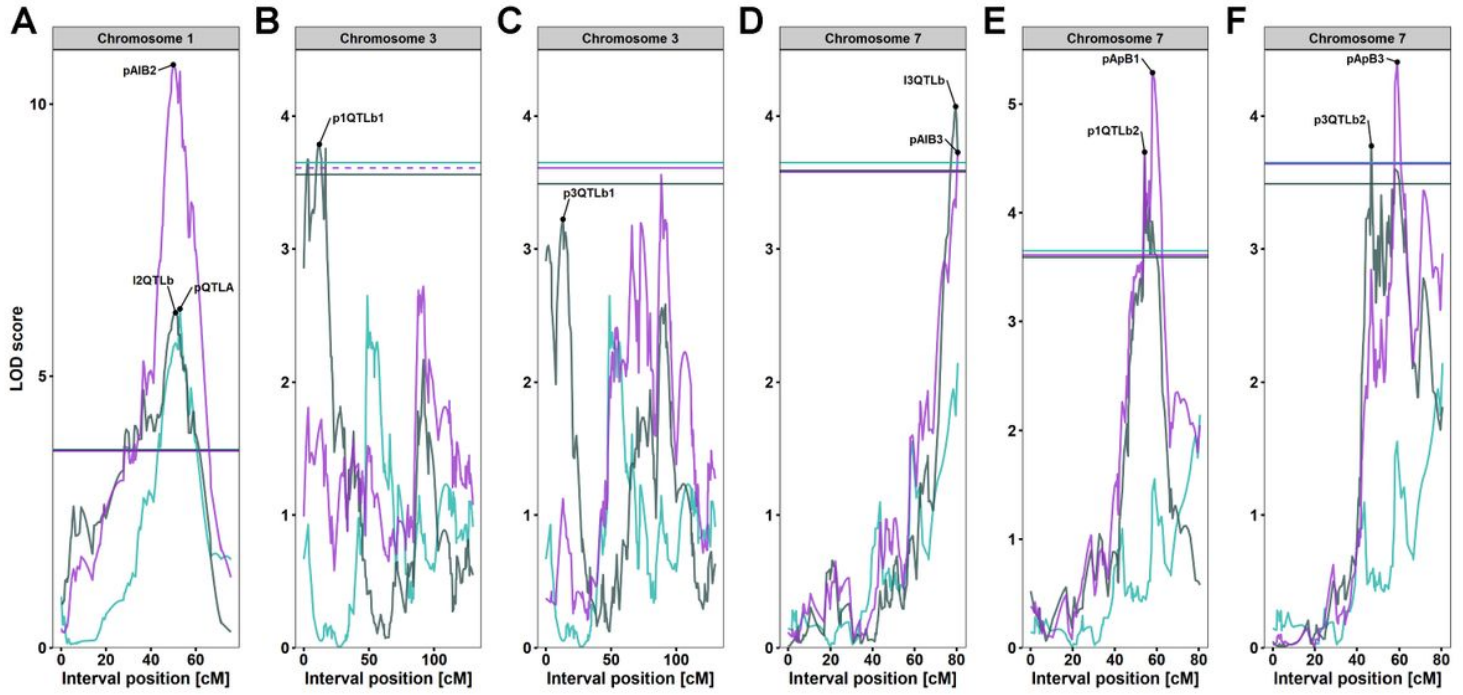

Figure 5

LOD-profiles for identified QTLs. Phenotypes from the petiole-assay in Population A were merged with QTL-phenotypes from Population B. Dark gray: LOD-profile from Population A; Turquoise: LOD-profile from Population B; Purple: LOD-profile for merged data from Population A and B. A Merged phenotypes from Population A and the 2nd leaf-assay in Population B (pAlB2). B-C Merged phenotypes from Population A with B the 1st and C 3rd petiole-assay in Population B. D Merged phenotypes from Population A with the 3rd leaf-assay (pAlB3). E-F Merged phenotypes from Population A with the E 1st petiole-assay and F 3rd petiole-assay in Population B.

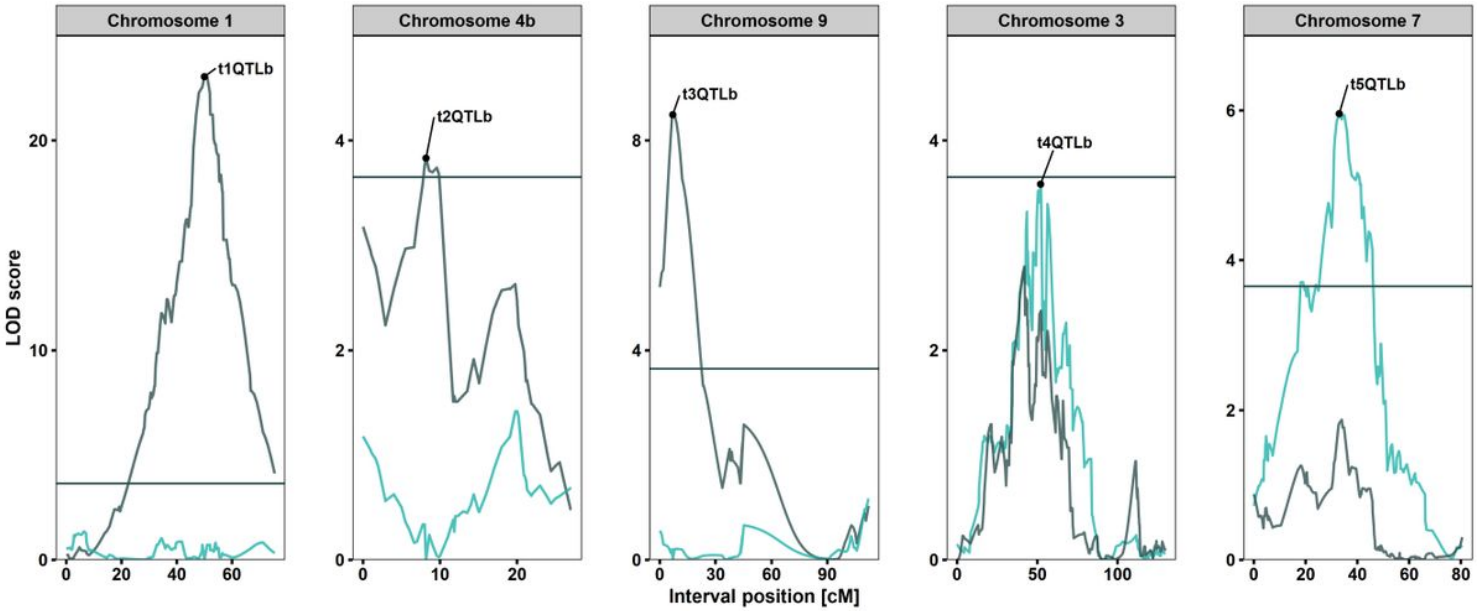

Figure 6

LOD-profiles for trichome-phenotypes in Population B. Dark gray: LOD-profiles from the one-dimensional scan; Turquoise: LOD-profile from the additional one-dimensional scan controlling for the QTLs on chromosomes C01, C04b, C09. Horizontal line indicates LOD-threshold.

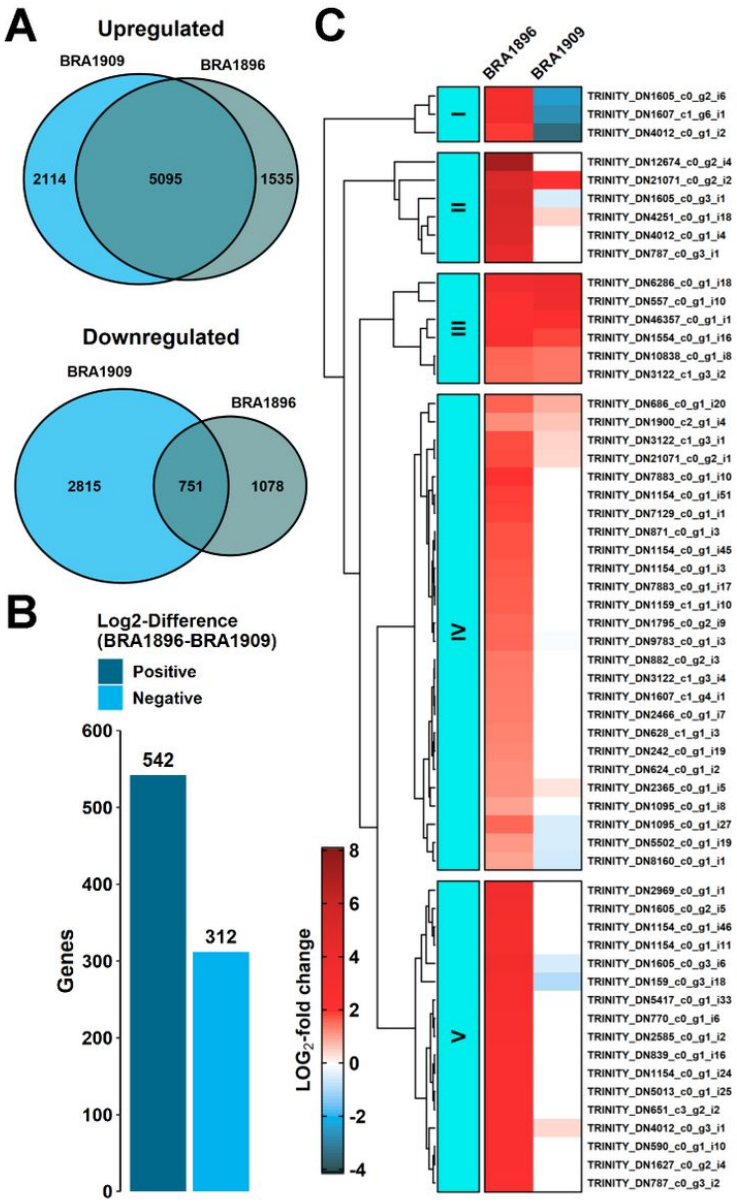

Figure 7

Main results of comparative RNAseq analyses. A Venn diagram of up- and downregulated DEGs in B. villosa (BRA1896) and B. oleracea (BRA1909). B Significantly differentially regulated genes between both species due to the Sclerotinia-inoculation. Positive: stronger induction in BRA1896; Negative: stronger induction in BRA1909. C Heatmap of significantly upregulated de novo transcripts specific to the resistant BRA1896 that are associated with defense response (GO: 0006952).

Supplementary Files

This is a list of supplementary files associated with this preprint. Click to download.

- SupplementaryFigures17.pdf
- SupplementaryData.xlsx
- TableS1.pdf